Physics – Uspekhi **49** (1) 69 – 87 (2006)

PHYSICS OF OUR DAYS

PACS numbers: **43.25.+y**, 62.20.Mk, **62.65.+k**

Giant nonlinearities in structurally inhomogeneous media and the fundamentals of nonlinear acoustic diagnostic techniques

O V Rudenko

DOI: 10.1070/PU2006v049n01ABEH005876

Contents

Abstract. The mechanisms responsible for anomalously strong acoustic nonlinearities in multiphase, defected, and structurally inhomogeneous media are summarized, and nonlinear diagnostics — a fast-growing applied area of recent years — is reviewed in terms of its methods and applications. This paper is an expanded version of the introductory talk at the September 18, 2005 session of the RAS Physical Sciences Division. An abridge version of other talks presented in the session is also given in this issue of *Physics – Uspekhi.*

1. Introduction

Nonlinear elastic properties of condensed media and the nonlinear waves therein have been extensively studied for over 50 years in the framework of a well-established discipline — nonlinear acoustics [1 – 3]. Recently, there has been an increasing interest in similar studies covering nonsingle-phase systems (gas – liquid media, granulated and fluid-saturated porous media, geological structures, gels, and composites), as well as solid bodies with defects and inhomogeneities on a mesoscopic (supramolecular) scale. This interest is in the first place due to the unusually strong nonlinearities in such media. It is often possible to observe markedly pronounced nonlinear phenomena in structurally inhomogeneous media at moderate sound intensities. This opens up the possibility for the development of highly sensitive nonlinear diagnostic technique and may have other implications.

It was previously thought that macroscopic elastic properties are formally determined by the power series expansion of the internal energy of a weakly deformed medium in terms of the strain invariants [4], coefficients of the quadratic terms of the expansion being linear moduli of elasticity and those of the cubic terms Landau's nonlinear moduli (or third-order moduli). Such nonlinearity is usually referred to as 'physical' [5] because it is due to the nonlinearity of intermolecular interaction forces in a condensed medium and, naturally, differs for various concrete media. This nonlinearity is responsible for many well-known phenomena, besides the effects of acoustic wave interaction, such as thermal expansion of bodies, deviation from the Dulong – Petit law at high temperatures, sound attenuation as a result of the interaction of coherent phonons with thermal noise (Landau – Rumer mechanism) [6], and some others.

Another type of nonlinearity is due to the nonlinear relation between components of the strain tensor and coordinate derivatives of the displacement vector components. This relation is independent of the physical properties of the body undergoing deformation and is called 'geometric' [5] nonlinearity.

It is worthwhile to recall how physical and geometric nonlinearities are distinguished in the equations of hydrodynamics [7]

$$\rho\left[\frac{\partial \mathbf{u}}{\partial t} + (\mathbf{u}\nabla)\mathbf{u}\right] = -\nabla p + \eta\Delta\mathbf{u} + \left(\zeta + \frac{\eta}{3}\right)\operatorname{grad}\operatorname{div}\mathbf{u}\,, \quad (1)$$

$$\frac{\partial \rho}{\partial t} + \operatorname{div}(\rho\mathbf{u}) = 0\,, \qquad p = p(\rho)\,, \quad (2)$$

where η and ζ are the shear and bulk viscosity coefficients, respectively. For simplicity, the change in entropy in the system (1), (2) is disregarded. Let the unperturbed state of a medium be $\rho = \rho_0$, $p = p_0$, and $\mathbf{u} = 0$. Let us further denote perturbations of the wave-associated parameters as ρ', p' and assume in Eqns (1), (2) that

$$\rho = \rho_0 + \rho'\,, \qquad p = p_0 + p'\,, \qquad \frac{\rho'}{\rho} \sim \frac{p'}{p_0} \sim \frac{|\mathbf{u}|}{c_0} \sim \mu \ll 1\,.$$

O V Rudenko M V Lomonosov Moscow State University, Vorob'evy Gory, 119992 Moscow, Russian Federation
Tel./Fax (7-495) 939 29 36
E-mail: rudenko@acs366.phys.msu.ru

Received 14 November 2005
Uspekhi Fizicheskikh Nauk **176** (1) 77 – 95 (2006)
Translated by Yu V Morozov; edited by A Radzig

Then, the equations of motion and continuity, retaining small terms of order μ^2, will have the form

$$\rho_0 \frac{\partial \mathbf{u}}{\partial t} + \nabla p' - \eta \Delta \mathbf{u} - \left(\zeta + \frac{\eta}{3}\right) \operatorname{grad} \operatorname{div} \mathbf{u} = -\rho' \frac{\partial \mathbf{u}}{\partial t} - (\rho_0 + \rho')(\mathbf{u}\nabla)\mathbf{u},$$

$$\frac{\partial \rho'}{\partial t} + \rho_0 \operatorname{div} \mathbf{u} = -\operatorname{div}(\rho' \mathbf{u}).$$

The left-hand sides of these equations contain linear terms, and their right-hand sides nonlinear ones. The latter appear by virtue of the nonlinearity of the initial equations and do not depend on the properties of the medium. Hence, the term geometric nonlinearity.

In contrast, series expansion of the equation of state:

$$p' = c_0^2 \rho' + \frac{1}{2}\left(\frac{\partial^2 p}{\partial \rho^2}\right) \rho'^2 + \ldots = C_1 \frac{\rho'}{\rho_0} + \frac{1}{2} C_2 \left(\frac{\rho'}{\rho_0}\right)^2 + \ldots \qquad (3)$$

leads to the appearance of nonlinear terms in the dependence interrelating increments of pressure and density; hence, the term physical nonlinearity.

For isotropic solids, the equation of motion and the relationship between the stress and strain tensors σ_{ik} and e_{ik} have the form

$$\rho_0 \frac{\partial^2 U_i}{\partial t^2} = \frac{\partial}{\partial x_k} \sigma_{ik},$$
$$\sigma_{ik} = K e_{ll} \delta_{ik} + 2\mu\left(e_{ik} - \frac{1}{3}\delta_{ik} e_{ll}\right) + O(e_{ik}^2), \qquad (4)$$

where U_i is the displacement vector, and K, μ are the bulk compression and shear moduli [4]; the strain tensor is defined as

$$e_{ik} = \frac{1}{2}\left(\frac{\partial U_i}{\partial x_k} + \frac{\partial U_k}{\partial x_i} + \frac{\partial U_l}{\partial x_k}\frac{\partial U_l}{\partial x_i}\right), \qquad (5)$$

and $O(e_{ik}^2)$ in formula (4) includes nonlinear terms describing deviations from the Hooke law:

$$O(e_{ik}^2) = \left(\mu + \frac{A}{4}\right)\left(\frac{\partial U_l}{\partial x_i}\frac{\partial U_l}{\partial x_k} + \frac{\partial U_i}{\partial x_l}\frac{\partial U_k}{\partial x_l} + \frac{\partial U_l}{\partial x_k}\frac{\partial U_i}{\partial x_l}\right) + \frac{1}{2}\left(K - \frac{2}{3}\mu + B\right)\left(\frac{\partial U_l}{\partial x_m}\frac{\partial U_l}{\partial x_m}\delta_{ik} + 2\frac{\partial U_i}{\partial x_k}\frac{\partial U_l}{\partial x_l}\right) + \frac{A}{4}\frac{\partial U_k}{\partial x_l}\frac{\partial U_l}{\partial x_i} + B\left(\frac{\partial U_l}{\partial x_m}\frac{\partial U_m}{\partial x_l}\delta_{ik} + 2\frac{\partial U_k}{\partial x_i}\frac{\partial U_l}{\partial x_l}\right) + C\frac{\partial U_l}{\partial x_l}\frac{\partial U_l}{\partial x_l}\delta_{ik}.$$

Here, A, B, and C are the nonlinear third-order moduli of elasticity (Landau coefficients [5] in the expansion of the internal energy in powers of strain tensors):

$$E = \mu e_{ik}^2 + \left(\frac{K}{2} - \frac{\mu}{3}\right) e_{ll}^2 + \frac{A}{3} e_{ik} e_{il} e_{kl} + B e_{ik}^2 e_{ll} + \frac{C}{3} e_{ll}^3.$$

Evidently, the geometric nonlinearity appears in dependence (5) of the strain tensor on displacement vector components, and the physical nonlinearity grows from all the terms in expression $O(e_{ik}^2)$ containing coefficients A, B, and C.

For liquids and gases, the coefficient of physical nonlinearity is usually introduced based on expansion (3): $\varepsilon_{\text{ph}} = C_2/2C_1$. The coefficient of geometric nonlinearity is $\varepsilon_{\text{g}} = 1$. The sum of these quantities

$$\varepsilon = \varepsilon_{\text{g}} + \varepsilon_{\text{ph}} = 1 + \frac{C_2}{2C_1} \qquad (6)$$

is simply called the coefficient of acoustic nonlinearity. For gases, this coefficient is expressed through the adiabatic index $\gamma = c_p/c_v$ as $\varepsilon = (\gamma + 1)/2$. Evidently, for air (a diatomic gas), $\varepsilon = 1.2$. In the case of liquids, ε is measured in experiment, e.g., from the generation of the second harmonic [1–3]. Typical values at 20 °C are $\varepsilon = 3.5$ (for distilled water), $\varepsilon = 5.6$ (acetone), and $\varepsilon = 6.3$ (alcohol).

It should be noted that the coefficient ε introduced by formula (6) enters principal mathematical models describing the propagation of nonlinear waves in liquids and gases — that is, in Riemann wave equations, Burgers and Khokhlov–Zabolotskaya equations, as well as in their various modifications [8].

Examples of such models are presented below. The general one-dimensional equation describing the propagation of diverging and converging waves (as in horns, acoustic concentrators, ray tubes in the approximation of nonlinear geometric acoustics) has the form

$$\frac{\partial p}{\partial x} + \frac{p}{2}\frac{\mathrm{d}}{\mathrm{d}x}\ln S(x) - \frac{\varepsilon}{c_0^3 \rho_0} p \frac{\partial p}{\partial \tau} - \frac{b}{2c_0^3 \rho_0}\frac{\partial^2 p}{\partial \tau^2} = 0, \qquad (7)$$

where $S(x)$ is the tube cross-section area, and $\tau = t - x/c_0$. The important specific cases are as follows: at $S(x) = \text{const}$, equation (7) transforms into Burgers equation for plane waves, $S(x) \sim x$ corresponds to cylindrical waves, and $S(x) \sim x^2$ to spherical ones. Dissipation (the second derivative) is associated with viscosity and heat conduction effects. A similar equation with the fourth derivative is used to take into account losses due to scattering by small inhomogeneities [9].

The integro-differential equation [2]

$$\frac{\partial p}{\partial x} - \frac{\varepsilon}{c_0^3 \rho_0} p \frac{\partial p}{\partial \tau} - \frac{m}{2c_0}\frac{\partial}{\partial \tau}\int_{-\infty}^{\tau} K(\tau - \tau')\frac{\partial p}{\partial \tau'}\,\mathrm{d}\tau' = 0 \qquad (8)$$

describes nonlinear waves in hereditary media. The important case of kernel $K(t) = \exp(-t/T)$ corresponds to the relaxing medium; power-like kernels are used for biological tissues, and models with several relaxation times for melts and highly viscous fluids.

The basic equation for intense acoustic beams is the Khokhlov–Zabolotskaya–Kuznetsov (KZK) equation [10]

$$\frac{\partial}{\partial \tau}\left[\frac{\partial p}{\partial x} - \frac{\varepsilon}{c_0^3 \rho_0} p \frac{\partial p}{\partial \tau} - \frac{b}{2c_0^3 \rho_0}\frac{\partial^2 p}{\partial \tau^2}\right] = \frac{c_0}{2}\Delta_{\perp} p, \qquad (9)$$

where $\Delta_{\perp}$ is the 'transverse' Laplace operator. The general construction of the equation for diffracting beams takes the form

$$\frac{\partial}{\partial \tau}\left[\hat{\Pi}(p)\right] = \frac{c_0}{2}\Delta_{\perp} p. \qquad (10)$$

Here, $\hat{\Pi}(p)$ is the left-hand side of the corresponding equation for one-dimensional waves [e.g., any one from Eqns (7), (8)].

The presence of quadratically nonlinear terms in these equations is associated with the appearance of a characteristic parameter — the nonlinear length

$$l_{\mathrm{NL}} = \frac{c_0^3 \rho_0}{\varepsilon \omega P_0} = \frac{\lambda}{2\pi\varepsilon M_\omega}\,, \tag{11}$$

where λ is the wavelength, and $M_\omega = P_0/c_0^2\rho_0$ is the acoustic Mach number for a wave with frequency ω. In the ideal case, i.e., when the nonlinearity predominates over competitive factors like damping, diffraction, etc., a discontinuity in the initial plane harmonic wave occurs (leading to shock front formation) at distance l_{NL} from the entrance to the medium. For example, $l_{\mathrm{NL}} \approx 25$ cm for a wave with the acoustic pressure amplitude $P_0 = 5.5 \times 10^5$ Pa (intensity 10 W cm^{-2}) and frequency 1 MHz in water. The amplitude P_2 of the second harmonic (without regard for the redistribution of its energy over higher harmonics) [8] would increase linearly with increasing x and would be as large as $0.5P_0$ at a distance $x = l_{\mathrm{NL}}$ (both experiments and the theory taking into consideration higher harmonics give a smaller value $P_2 = J_2(2)P_0 \approx 0.35P_0$, where J_2 is the Bessel function). Thus, the simplest way to estimate the nonlinear parameter ε boils down to determining the nonlinear length or to measuring the amplitude P_2 of the second harmonic at small distances $x \leqslant 0.5 l_{\mathrm{NL}}$:

$$\varepsilon = \frac{2c_0^3\rho_0}{\omega x}\frac{P_2}{P_0^2} = \frac{1}{\pi N}\frac{M_{2\omega}}{M_\omega^2}\,, \tag{12}$$

where $N = x/\lambda$ is the number of the wavelengths being along the distance x. There are many other methods to estimate ε based on the measurement of spatio-temporal and spectral characteristics of running waves and on resonance phenomena (see Refs [1–3, 11–13]). Resonance methods were extensively employed in biomedical studies [14, 15] that require high-precision measurement of physical nonlinearity for the correct evaluation of conditions of tissues, organs, and body fluids.

In solids, waves of different types can interact, which accounts for the lack of a universal expression for nonlinear coefficient (6). In the specific case of plane longitudinal waves propagating in an isotropic medium [1], one finds

$$\varepsilon = -\frac{3}{2} - \frac{1}{c_0^2\rho_0}(A + 3B + C)\,.$$

As shown by measurements, ε for homogeneous bodies exhibits the same order of magnitude as for liquids (e.g., $\varepsilon = 7.2$ for aluminium) and rarely exceeds 10.

However, many experiments in structurally inhomogeneous media have given values of $\varepsilon \sim 10^2 - 10^3$. The underlying causes of such large values differ from those discussed above in connection with physical and geometric nonlinearities. This provides grounds for distinguishing nonlinearity of a third type, called 'structural' nonlinearity.

2. Classification of acoustic nonlinearities

It follows from the foregoing section that there is good reason to consider three types of nonlinearity, viz. geometric, physical, and structural, each being either dispersed in a bulk medium or concentrated in a spatial domain that is small compared with the wavelength [16]. Effects of bulk nonlinearities may accumulate during wave propagation (provided competitive processes, such as damping, diffraction, dispersion, etc. are sufficiently weak). These effects tend to manifest themselves more strongly the longer the distance travelled by the wave. They can be very pronounced even in the case of weak nonlinearity. In contrast, the accumulation of effects of boundary nonlinearity is feasible only in the case of repeated action of the wave on the nonlinear element (boundary), e.g., when this element is enclosed in a resonator.

Let us discuss examples of boundary nonlinearities.

Example 1. Geometric boundary nonlinearity. Let us consider a flat piston whose vibration along the normal (coincident with the x-axis) to its surface excites a running wave in an elastic half-space $x > 0$. A displacement of the piston from the mean position $x = 0$ is described by the law $x = X(t)$. A wave moving away from the piston imparts the velocity to medium particles varying as $u = u_0\Phi(t - x/c)$.

Because the speed of the piston surface equals the velocity of medium particles residing at this surface, one arrives at a functional equation for unknown Φ:

$$\frac{\mathrm{d}X}{\mathrm{d}t} = u_0\Phi\left(t - \frac{X(t)}{c}\right), \tag{13}$$

the solution of which [17] nonlinearly depends on the known function $X(t)$:

$$\Phi(t) = \frac{1}{2\pi \mathrm{i}}\int_{-\infty}^{\infty}\exp(\mathrm{i}\omega t)\,\frac{\mathrm{d}\omega}{\omega} \times \int_{-\infty}^{\infty}\frac{\mathrm{d}^2X}{\mathrm{d}\xi^2}\exp\left[\mathrm{i}\,\frac{\omega}{c}\,X(\xi) - \mathrm{i}\omega\xi\right]\mathrm{d}\xi\,. \tag{14}$$

For example, if the piston movements conform to the harmonic law $X(t) = -X_0\cos\omega t$, Eqn (13) takes the form

$$\frac{u}{u_0} = \Phi\left(\omega t + \frac{u_0}{c}\cos\omega t\right) = \sin\omega t\,, \qquad u_0 = \omega X_0\,. \tag{15}$$

Evidently, the shape of the running wave $\Phi(t)$ contains both a constant constituent and higher harmonics in the case of the harmonic dependence $X(t)$. The difference between $X'(t)$ and $\Phi(t)$ increases with an increasing Mach number $M = u_0/c$ and becomes especially apparent at the speeds of piston motion comparable with the speed of sound. Such a situation may arise in liquids containing gas bubbles in which the speed of sound may be very low, and also in resonators where boundary nonlinearity effects may accumulate in the course of time. Because the nonlinearity of relation (13) is independent of the medium's properties, it would be worthwhile to call this nonlinearity geometric.

The shape of wave (15) at small Mach numbers is close to sinusoidal, and its positive and negative 'half-periods' are differently distorted at finite M — that is, the phase of positive u values is shortened in time and has a higher maximum compared with the absolute maximum of the phase of negative u values. Spectral components (14) of this wave are defined by the Fourier series expansion:

$$\frac{u}{u_0} = \Phi(\omega t) = \sum_{n=0}^{\infty}\frac{\mathrm{i}^{-n}}{n}\,J'(nM)\exp(\mathrm{i}n\omega t) = \sum_{n=0}^{\infty}(A_n\cos n\omega t + B_n\sin n\omega t)\,. \tag{16}$$

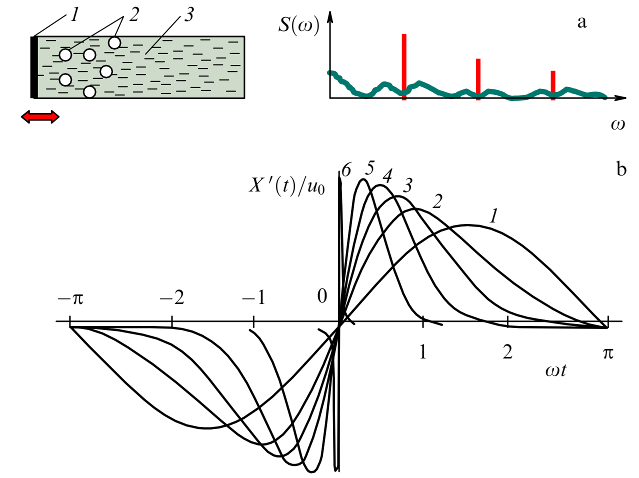

Figure 1. (a) Broadening of the spectrum $S(\omega)$ of cavitation noise interacting with the boundary (*1*) vibrating in accordance with the harmonic law; *2* — cavitation bubbles, and *3* — fluid. (b) The shape of one boundary oscillation period that ensures accumulation of energy in the resonator cavity under conditions of manifestation of the boundary nonlinearity. Curves *1* – *6* correspond to increasing u_0 values.

Specifically, for the constant constituent and amplitudes of the first two harmonics, one obtains

$$A_0 = -\frac{M}{2}\,,$$
$$B_1 = J_0(M) - J_2(M)\,, \tag{17}$$
$$A_2 = -\frac{1}{2}\left[J_1(2M) - J_3(2M)\right].$$

The constant constituent of the velocity is directed toward the piston. It appears in connection with the representation of the vibrating boundary as an infinite plane: the pressure in any direction orthogonal to x being identical (unlike the pressure in the case of a piston of finite size), the fluid cannot approach the axis (see, for instance, problem 4 in Ref. [7, § 101]).

Thus, geometric boundary nonlinearity effects do not depend on the properties of the medium or the distance travelled by the wave — they are heightened with increasing Mach number M.

Geometric boundary nonlinearity may become apparent when a cloud of cavitation bubbles forms in the fluid close to a high-power ultrasonic source. The speed of sound in such a medium is sometimes reduced to 20 – 40 m s^{-1}. The bubbles vibrate, collapse, and produce broadband noise. This noise interacts with boundary vibrations, and its spectrum is reproduced at the 'base' of discrete constituents, i.e., higher harmonics of the fundamental frequency (Fig. 1a). As a result, the noise builds up, and the spectrum effectively broadens [17]. The mechanism described adds to the known mechanisms [6] of spectrum broadening under the influence of bulk nonlinearity.

Other problems that require consideration of the finiteness of the boundary displacement are related to the accumulation of nonlinear distortions in high-Q resonators. Because the shape of intense 'standing' waves is greatly distorted, they become saturated under harmonic pumping. Therefore, the form of boundary vibrations needs to be altered [18] if the process of 'pumping' energy into the resonator is to be continued (in analogy with increasing the time interval between consecutive pushes to keep pumping a child's swing). The form of the wall motion (one period) necessary to maintain resonant excitation is shown in Fig. 1b. Interestingly, resonance in a system with boundary nonlinearity is observed in frequency bands that broaden with increasing boundary vibration amplitude, rather than at certain discrete eigenfrequencies [19].

Example 1a. This example illustrates nonlinearity of the same type as the example 1 but concerns well-known devices, such as resonance sound absorbers utilized to reduce noise in building construction. A resonance sound absorber is essentially a perforated plate attached to a wall from which it is separated by a narrow gap. Such a device is equivalent to a system of Helmholtz resonators, with each hole functioning as a resonator 'neck', and the air enclosed in the gap behind it as a virtually motionless compressible volume. Vibrations of air in the holes are damped out by virtue of friction against the hole walls or nets and special fibrous material enclosed in them. The correct choice of resonator parameters at a certain frequency allows having the incident waves be completely absorbed. Nonlinearity may weaken the damping effect of an absorber tuned to be resonant with certain linear parameters or, vice versa, improve sound absorption by a poorly tuned system by setting it closer to exact resonance [20]. In other words, it is necessary to take into account boundary nonlinearity effects when devising intense sound absorbers. The nature of this nonlinearity bears a general character; it manifests itself when an oscillating stream flows around a sharp-edged body. In such a case, the flux gradients are on the order of $u/\max(r_0, \delta)$, where $\delta = \sqrt{\nu/\omega}$ is the thickness of the acoustic boundary layer, r_0 is the minimal radius of the obstacle curvature, and ν is the kinematic viscosity. Thickness δ determines decisively the behavior of the stream as it flows round the sharp-edged body. The nonlinearity is essential when the Reynolds number $\mathrm{Re} \sim 1$ is proportional to the ratio of the terms on the left-hand side of the equation of motion (1) that can be evaluated as

$$\mathrm{Re} \sim \left| (\mathbf{u}\nabla)\,\mathbf{u} \left(\frac{\partial \mathbf{u}}{\partial t} \right)^{-1} \right| \sim \frac{u}{\sqrt{\omega\nu}} = \sqrt{\frac{2I}{c\omega\eta}}\,, \tag{18}$$

where I is the sound intensity. In accordance with estimate (18), the nonlinearity in the air ($\eta = 0.018 \times 10^{-3}$ Pa s) is apparent at 500 Hz when the sound intensity reaches ~ 120 dB. This estimate agrees with experimental data. If vortices are induced at the hole edges, nonlinear phenomena can be observed even beginning with the sound intensity of 90 dB [20].

Example 2. Physical boundary nonlinearity. In many problems, the known variable is a force $F(t)$ applied to the piston rather than the piston displacement law $x = X(t)$ as in example 1a. Thus, when an alternating voltage V is fed to an electromechanical transducer, it is the law $V(t)$ that is known and, consequently, $F(t)$. The equation for the vibrations of a piston having mass m and surface area S, namely

$$m\,\frac{\mathrm{d}^2 X}{\mathrm{d}t^2} = F(t) - p_{\mathrm{a}} S\,, \tag{19}$$

takes into account the response of p_{a}, i.e., pressure produced by the runaway wave. This pressure is related to the vibrational velocity u by the nonlinear relation $p_{\mathrm{a}} = p_{\mathrm{a}}(u)$ known from the theory of Riemann waves [7]. Because $u = X'(t)$ at the piston surface, we must set $p_{\mathrm{a}} = p_{\mathrm{a}}(\mathrm{d}X/\mathrm{d}t)$ in Eqn (19). If the nonlinearity is weak and we may restrict

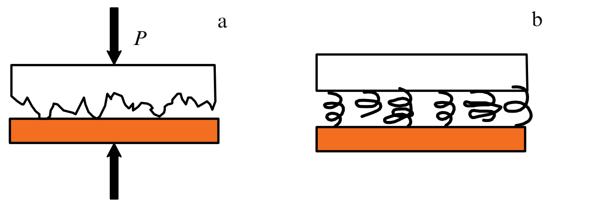

Figure 2. (a) Schematic representation of a rough surface. (b) Model of a rough surface in the form of an ensemble of springs with different lengths and equal rigidity.

ourselves to a quadratic nonlinear relation, then equation (19) takes the form

$$\frac{\mathrm{d}^2 X}{\mathrm{d}t^2} + \frac{c\rho S}{m}\frac{\mathrm{d}X}{\mathrm{d}t}\left(1 + \frac{\varepsilon}{2c}\frac{\mathrm{d}X}{\mathrm{d}t}\right) = \frac{1}{m}F(t)\,. \tag{20}$$

It is clear that the response of the runaway wave to the piston action is also nonlinear. If $F(t)$ varies according to the harmonic law, then function $X(t)$ contains higher harmonics. The nonlinearity tends to manifest itself more strongly the larger the product of the medium nonlinear parameter and the Mach number, namely, εM. The response is due to the nonlinear dependence of pressure on the velocity or the excitation of medium density (in solids, the nonlinear stress – strain relation can be discussed). For this reason, the above-described nonlinearity may be called physical nonlinearity.

Example 3. Structural boundary nonlinearity. Figure 2a depicts a system of two plates, one of which (bottom) is smooth, and the other rough. Evidently, the larger the pressing force P, the more the 'teethes' (i.e., microscopic asperities at the contact sites) undergo distortion and the rigidity of the contact increases.

Structural nonlinearity is evidenced in a simple experiment [21] schematically represented in Fig. 3. In this case, the structural nonlinearity can be used to estimate the quality of two rough surfaces in contact [22]. As $P \to 0$, the incident wave with frequency ω is almost completely reflected from the interface. Conversely, if $P \to \infty$, the wave passes across the interface due to ideal acoustic contact. In either case, there is no reflected wave at frequency 2ω. The second harmonic arises at intermediate P values, while the P-dependence of the displacement amplitude $U_{2\omega}$ has a maximum. Interestingly, the curve $U_{2\omega}(P)$ represents the statistical distribution of microasperity heights [22] (in the framework of the model shown in Fig. 2b).

The contact nonlinearity has already been exploited in measuring and realizing interactions between bulk and surface waves of various types (e.g., in acoustoelectronic devices for signal processing). The term 'contact acoustic nonlinearity' (CAN) has been coined. These issues are discussed at greater length in Ref. [24].

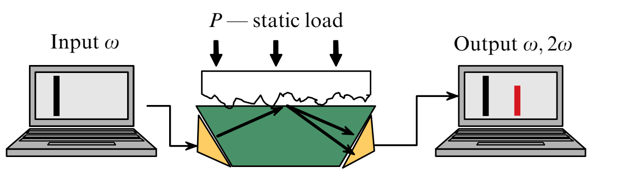

Figure 3. Rough surface diagnostics based on the generation of harmonics arising due to structural nonlinearity.

The magnitude of the signal generated as a result of the reflection from a nonlinear element depends on a variety of parameters. Therefore, one should be cautious when speaking of 'giant medium nonlinearities'. Let us discuss, by way of example, the problem of acoustic wave reflection in the simplest one-dimensional representation. Let the displacement $X(t)$ of an element at point $x = 0$ under the action of acoustic pressure be described by the equation $\hat{L}(X) = p_{\mathrm{a}}(t)$, where the pressure field is the sum of the incident (from $-\infty$) and reflected waves:

$$p_{\mathrm{a}}(x,t) = p_+\left(t - \frac{x}{c}\right) + p_-\left(t + \frac{x}{c}\right).$$

The following system is needed to obtain the reflected wave:

$$\rho c\,\frac{\mathrm{d}X}{\mathrm{d}t} + \hat{L}(X) = 2p_+(t)\,, \qquad p_- = p_+ - \rho c\,\frac{\mathrm{d}X}{\mathrm{d}t}\,.$$

Specifically, for a harmonic incident wave and weak inertialess quadratic nonlinearity $\hat{L}(X) = E(1 + \varepsilon X/h)X/h$ (where E, ε are the Young modulus and the coefficient of the material nonlinearity, respectively, and h is the thickness of the nonlinear layer), the following relations hold:

$$\frac{M_{2\omega}}{M_\omega^2} = 4\,\frac{c^2\rho}{E}\,\frac{G}{1+G^2}\,\frac{1}{\sqrt{1+4G^2}}\,\varepsilon\,, \qquad G = \frac{\omega}{c}\,h\,\frac{c^2\rho}{E}\,. \tag{21}$$

It can be seen that the ratio of the Mach number of the second harmonic to the Mach number squared of the first harmonic can grow not only with increasing nonlinear parameter ε but also with growing ratio $c^2\rho/E$ of compressibilities of the nonlinear material and the 'buffer' medium in which the incident signal is excited and the reflected one is registered.

It appears from the comparison of Eqn (21) in the limiting case of low frequencies (for small G values) with the analogous expression (12) for bulk nonlinearity that the coefficient of ε in equation (21) contains the product of the small wave layer thickness and the square of the compressibility ratio $4kh(c^2\rho/E)^2$, instead of the number πN of wavelengths. If the nonlinear element has a linear Young modulus smaller than the modulus for the 'buffer' medium, then it is more appropriate to speak about the strong manifestation of weak nonlinearity rather than of strong nonlinearity.

An example is provided by the response of a thin gas layer $(\rho_{\mathrm{G}}, c_{\mathrm{G}})$ residing in a liquid $(\rho_{\mathrm{L}}, c_{\mathrm{L}})$ medium (Fig. 4). The exact solution of the problem of harmonic signal reflection from the layer [whose density shows the dependence on acoustic pressure simulated by the expression $c^2\rho/p_* = \ln(1 + p/p_*)$] has the form [25]

$$\frac{p}{p_*} = \exp\left(-\frac{\zeta}{\Delta}\cos\omega t\right) \times \left[I_0\left(\frac{\zeta}{\Delta}\,b\right) + 2\sum_{n=1}^{\infty}(-1)^n I_n\left(\frac{\zeta}{\Delta}\,b\right)\frac{\zeta}{\sqrt{\zeta^2 + n^2\Delta^2}} \times \cos\left(n\omega t - \arctan\frac{\zeta}{\Delta}\right)\right]^{-1} - 1\,, \tag{22}$$

where I_0, I_n are the modified Bessel functions. This relationship contains the ratio of two small parameters $\zeta = \rho_{\mathrm{G}} c_{\mathrm{G}}/(\rho_{\mathrm{L}} c_{\mathrm{L}})$ and $\Delta = \omega h/2c_{\mathrm{L}}$. The curves in Fig. 4a are

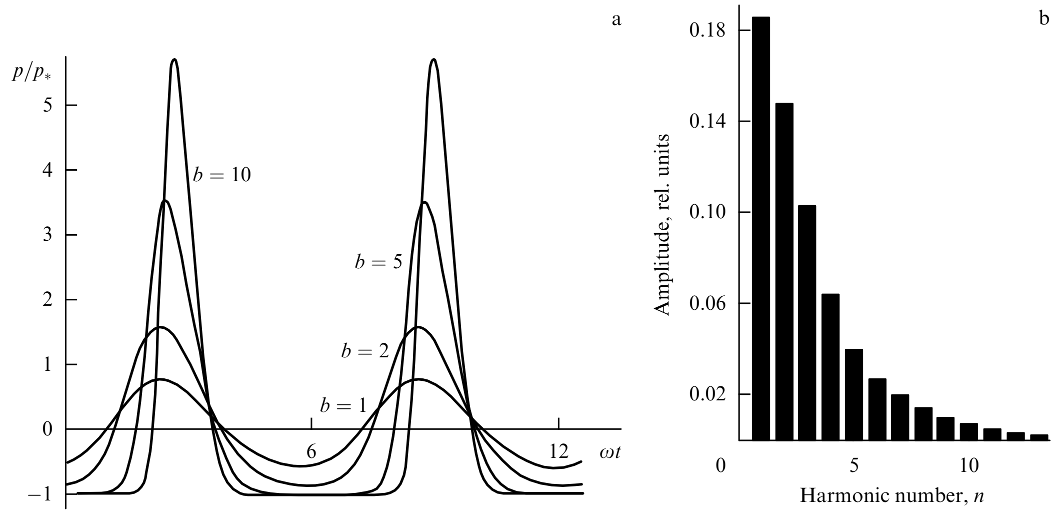

Figure 4. (a) The shape of a time-periodic, strongly nonlinear response of the layer at different b values, and (b) the spectrum of the response at $b = 10$.

constructed for the ratio $\zeta/\Delta = 1$ and the values of the parameter $b = P_0/p_*$ equal to 1, 2, 5, and 10. It can be seen that nonlinear distortions are amplified with increasing b. The reflected spectrum at $b = 10$ (Fig. 4b) contains some dozen harmonics of the incident wave frequency. As shown in Ref. [25], processing the broad spectrum of a reflected signal permits us to solve the inverse problem, i.e., to reconstruct the equation of state of the layer.

As distinct from a separate weakly nonlinear element responsible for the strong nonlinear response, a distributed system composed of such elements can be appropriately described in such terms as 'strong' and even 'giant' nonlinearity because, in this case, effective elastic characteristics of a structurally inhomogeneous medium are involved.

This does not refer to individual elements that display strongly nonlinear behavior even under weak acoustical action. The examples are nonlinearities inherent in systems with couplings and constraints (see Section 3 for 'clapping' nonlinearity) as well as in systems subjected to shocks or containing singularities in the equation of state. Such systems may be lacking in linear regime even when a small deviation from equilibrium exists. If a medium contains an ensemble of such strongly nonlinear elements, there is all the more reason to apply to it the term 'giant nonlinearity'.

3. Mechanisms of structural nonlinearity

Let us discuss here some causes that lead to the appearance of large bulk nonlinearities in structurally inhomogeneous media.

This type of nonlinearity arises in liquids into which strongly compressible inclusions are introduced (e.g., gas bubbles); it is known that the nonlinear parameter of aerated water may by two or three orders of magnitude exceed the nonlinearity of each constituent component of the mixture: gas ($\varepsilon = 1.2$) and water ($\varepsilon = 3.5$) alike.

Such nonlinearities have many times been observed and used to realize various acoustic interactions in liquids (see, for instance, Refs [26 – 30]). Large nonlinearities of vapor – liquid and gas – liquid systems are typical of a variety of wave problems in mechanics and thermal physics [31, 32].

Giant nonlinearity of liquids containing gas bubbles opened up possibilities to solve some applied problems, such as the detection of a small number of bubbles (and even single ones) in the wake of a seagoing ship, monitoring fermentation processes or the start of boiling of a coolant in nuclear reactors, diagnosis of decompression sickness, etc. It has also been suggested that the bubble-containing fluid nonlinearity be used in different industrial technologies. In the 1980s, extensive studies along these lines were carried out at the Institute of Applied Physics, Russian Academy of Sciences [33, 34]. At present, medical diagnostic technologies are being increasingly developed using stable microbubble-based suspensions (special contrast agents) for intravenous administration (see Section 5).

Markedly enhanced nonlinearity of media containing strongly compressible inclusions is illustrated by the following simple example. Let a thin layer of a light compressible medium be imbedded in a denser medium characterized by a high velocity of sound (for instance, a thin layer of air in water or aqueous gel). There are two small parameters in such a system: the acoustic impedance ratio, and the wave layer thickness $\rho_G c_G/\rho_L c_L \sim \omega h/c_G \ll 1$. The solution of the problem of wave passage through this layer [25] indicates that the second harmonic at the exit from it is $K \gg 1$ times stronger when the light layer is surrounded by a dense medium (compared with the second harmonic in the absence of a dense medium). The magnitude of 'enhancement' of nonlinearity, required for the generation of the second harmonic, comes out to

$$K = \frac{P_2^{\text{inh}}}{P_2^{\text{hg}}} = \frac{2}{3}\frac{\varepsilon_G}{\varepsilon_L}\left(\frac{c_L^2 \rho_L}{c_G^2 \rho_G}\right)^2 . \tag{23}$$

For the air layer in water, one obtains $K \approx 5.5 \times 10^7$. A layer composed of water containing bubbles at a bulk concentration of about 10^{-4} produces a 5000-fold enhancement.

There is a very simple explanation for the giant enhancement of nonlinearity. Let a wave propagate in a water layer with a characteristic pressure of several atmospheres. Such a wave is weak because the internal pressure $c_L^2 \rho_L$ in water is on the order of 23,000 atmospheres. However, when such pressure begins to act on the air layer, its volume changes several times and the resulting strong deformation leads to harmonic generation.

Despite the apparent simplicity of this phenomenon, no acceptable theory has thus far been proposed to quantitatively estimate the maximum values of the nonlinearity parameter in gas–liquid media. Formula (23) was derived from a too much simplified model and therefore gives only an upper bound. It is possible, following Ref. [30], to consider the dynamics of a single bubble and thereafter move to a fluid containing an ensemble of bubbles (nonlinear oscillators). The equation for bubble vibrations in an acoustic pressure field $p(t)$ in a liquid is derived from the Rayleigh equation [7] and, with allowance for gas compressibility inside a bubble, has the form

$$\frac{\mathrm{d}^2 w}{\mathrm{d}t^2} - \frac{1}{6}\left[2w\,\frac{\mathrm{d}^2 w}{\mathrm{d}t^2} + \left(\frac{\mathrm{d}w}{\mathrm{d}t}\right)^2\right] + \omega_0^2 w(1-\varepsilon_{\mathrm{G}} w) = -\omega_0^2\,\frac{p(t)}{c_{\mathrm{G}}^2\,\rho_{\mathrm{G}}}\,. \tag{24}$$

Here, w, ω_0^2 are the relative perturbation of the bubble volume and the square of eigenfrequency of its linear vibrations:

$$w = \frac{V'}{V_0}\,, \qquad \omega_0^2 = \frac{3c_{\mathrm{G}}^2}{R_0^2}\,\frac{\rho_{\mathrm{G}}}{\rho_{\mathrm{L}}}\,, \tag{25}$$

where V_0, R_0 are the equilibrium volume of a spherical bubble and its radius, and ε_{G} is the gas nonlinear parameter (6). In accordance with formulas (25), the resonant wavelength of the wave is much larger than the bubble radius because the oscillator has weak compressibility (gas) and a large virtual mass of the covibrating fluid. For example, the wavelength in water at a frequency of 1 MHz reaches 1.5 mm, while the 'resonant' bubble radius is only 4 μm.

Equation (24) contains both geometric nonlinearity (the term in square brackets appearing in the Rayleigh equation because of the nonlinearity of the Euler equation) and physical nonlinearity proportional to ε_{G}. Their ratio is a value on the order of $\omega^2/(2\varepsilon_{\mathrm{G}}\omega_0^2)$, where ω is the frequency of acoustic vibrations. Thus, the physical nonlinearity for low-frequency (nonresonant) bubbles markedly exceeds the geometric one; therefore, the latter may be neglected. It is the large nonlinear low-frequency response related to strong gas compressibility in a bubble that provides a basis for nonlinear diagnostics of separate microbubbles. As the frequency approaches the resonance one, the linear scattering predominates, and the resonance scattering cross section is $4/(kR_0)^2$ times the bubble cross section (the relative increase for a bubble in water is around 2×10^4 [35]).

Retaining only the nonlinear term $\sim\varepsilon_{\mathrm{G}}$ in Eqn (24) and supplementing it by the wave equation for acoustic pressure (derived from linearized equations of hydrodynamics for a liquid with the effective density $\rho = \rho_{\mathrm{L}}(p)\big(1 - nV(p)\big)$, where n is the number of bubbles per unit volume) it is possible to obtain the system of equations [30]

$$\frac{\mathrm{d}^2 w}{\mathrm{d}t^2} + \omega_0^2 w(1-\varepsilon_{\mathrm{G}} w) = -\omega_0^2\,\frac{p(t)}{c_{\mathrm{G}}^2\,\rho_{\mathrm{G}}}\,, \tag{26}$$

$$\Delta p - \frac{1}{c_{\mathrm{L}}^2}\,\frac{\partial^2 p}{\partial t^2} = -\rho_{\mathrm{L}} n V_0\,\frac{\partial^2 w}{\partial t^2}\,. \tag{27}$$

System (26), (27) coincides with the equations used in nonlinear optics of dielectrics [36], where p is the electric field, and w is the polarization of the medium in the Drude–Lorentz type model. This system is convenient to use for the solution of the problem of maximum nonlinearities.

Putting aside resonant phenomena, let us neglect the second derivative in equation (26). In this case, the effective low-frequency speed of sound

$$c_{\mathrm{eff}}^2 = \frac{c_{\mathrm{L}}^2}{1 + nV_0\,\beta}\,, \qquad \beta = \frac{c_{\mathrm{L}}^2\,\rho_{\mathrm{L}}}{c_{\mathrm{G}}^2\,\rho_{\mathrm{G}}}\,, \tag{28}$$

falls with the growth in both the gas content nV_0 and the ratio of medium compressibilities β. System (26), (27) is weakly dispersive and can be reduced to the Riemann wave equation by the method of slowly changing profile [36] [cf. Eqn (7)]:

$$\frac{\partial p}{\partial x} - \frac{\varepsilon_{\mathrm{eff}}}{c_{\mathrm{eff}}^3\,\rho_{\mathrm{eff}}}\,p\,\frac{\partial p}{\partial \tau} = 0\,, \qquad \frac{\varepsilon_{\mathrm{eff}}}{c_{\mathrm{eff}}^3\,\rho_{\mathrm{eff}}} \equiv \varepsilon_{\mathrm{G}} c_{\mathrm{eff}}\,\frac{\rho_{\mathrm{L}} n V_0}{(c_{\mathrm{G}}^2\,\rho_{\mathrm{G}})^2}\,, \tag{29}$$

where $\tau = t - x/c_{\mathrm{eff}}$ is the time in the coordinate system comoving the wave. Whence, the effective nonlinearity coefficient is defined as

$$\frac{\varepsilon_{\mathrm{eff}}}{\varepsilon_{\mathrm{G}}} = \frac{\beta^2 nV_0(1-nV_0)}{(1+\beta nV_0)^2}\,. \tag{30}$$

It can be seen that the maximum nonlinearity

$$\varepsilon_{\mathrm{eff}} = \varepsilon_{\mathrm{G}}\,\frac{\beta^2}{4(\beta+1)} \tag{31}$$

is achieved at a gas content $nV_0 = (\beta+2)^{-1}$. Estimates for a two-phase system consisting of water and air bubbles indicate that the effective nonlinearity may increase by $K = \varepsilon_{\mathrm{eff}}/\varepsilon_{\mathrm{G}} \approx 3900$ times compared with that of a diatomic gas and reach a maximum value $\varepsilon_{\mathrm{eff}} \approx 4700$ at a relative bulk content of the gas as small as 0.7×10^{-4}.

The above values are consistent with the results of many measurements and also with an estimate obtained from formula (23). At the same time, things are far from completely clear. In a previous consideration, the bubble was regarded as an oscillator free from losses, deformations were assumed to be finite but small, while scattering and some other factors were disregarded. One would think that the issue of maximum $\varepsilon_{\mathrm{eff}}$ could be solved in principle by considering a one-dimensional problem of periodically alternating plane-parallel layers of two media, $\rho_{\mathrm{G}}c_{\mathrm{G}}$, $\rho_{\mathrm{L}}c_{\mathrm{L}}$, of thickness h_{G}, h_{L}. In the linear formulation, such a problem was resolved long ago (see, for instance, Refs [36, 37]). The corresponding dispersion equation

$$\cos\big(k_{\mathrm{eff}}(h_{\mathrm{G}}+h_{\mathrm{L}})\big) = \cos(k_{\mathrm{G}}h_{\mathrm{G}})\cos(k_{\mathrm{L}}h_{\mathrm{L}}) - \frac{1}{2}\left(\frac{k_{\mathrm{G}}}{k_{\mathrm{L}}} + \frac{k_{\mathrm{L}}}{k_{\mathrm{G}}}\right)\sin(k_{\mathrm{G}}h_{\mathrm{G}})\sin(k_{\mathrm{L}}h_{\mathrm{L}}) \tag{32}$$

results from joining the solutions of the wave equation at the boundaries for each layer. In the long-wave approximation, it follows from Eqn (32) that

$$\frac{h_{\mathrm{G}}+h_{\mathrm{L}}}{c_{\mathrm{eff}}^2} = \frac{h_{\mathrm{G}}}{c_{\mathrm{G}}^2} + \frac{h_{\mathrm{L}}}{c_{\mathrm{L}}^2}\,. \tag{33}$$

For $c_{\mathrm{G}}^2 \ll c_{\mathrm{L}}^2$, formula (33) yields an incorrect result being in conflict with experimental findings. For example, it gives the speed of sound as high as 235 m s^{-1}, much in excess of 30–100 m s^{-1} in a system with equally thick layers of water and air. The fact is, classical theory (32) does not take into consideration boundary displacements that are essential in the case of high compressibility of the air, i.e., boundary nonlinearity (see example 1 in Section 2). The correct result obtained in the framework of the quasistatic approach (Mallock's formula [31]) is given by

$$\frac{(h_G + h_L)^2}{h_G h_L}\,\frac{1}{c_{\rm eff}^2} = \frac{\rho_L}{\rho_G}\,\frac{1}{c_G^2} + \frac{\rho_G}{\rho_L}\,\frac{1}{c_L^2}\,; \tag{34}$$

it indicates that the minimal possible speed $c_{\rm eff} = 23.8$ m s^{-1} in the case of equally thick layers, $h_G = h_L$, is much lower than the speed of sound in either water or air. One order of magnitude difference between the linear problem solution and the real data due to disregarding boundary displacements illustrates the difficulties of a strict solution of the problem in the 'physically nonlinear' formulation.

In addition to the lack of a clear and definite answer to the question concerning the magnitude of nonlinear moduli, there is an equally important question of how large the Reynolds acoustic numbers [1–3] that characterize the relative contributions of nonlinear effects and competing decays (due to wave dissipation, reflection, scattering, etc.) may be. It is not infrequent that the growth of nonlinearity is accompanied by still greater losses which hinder taking measurements.

Let us now turn to structurally inhomogeneous solid media. As shown in many experiments, an enhancement in nonlinearity K in such media (granulated, fluid-saturated, cracked, porous, etc.) may be as large as $10^2 - 10^4$. In this case, a rise in K suggests the presence of defects.

Media possessing strongly nonlinear properties are exemplified by a granulated system. The contact area between granules depends on the exerted force; in other words, the system is being deformed as an ensemble of nonlinear springs. An example is provided by the classical contact problem of the theory of elasticity, viz., the problem of two spheres (the Hertz contact) [4] (Fig. 5). The force by which two spheres of radii R_1 and R_2 are repulsed from each other nonlinearly depends on the difference between the displacements $(\xi_2 - \xi_1)$ of their centers under the strain effect:

$$F = E\sqrt{\frac{R_1 R_2}{R_1 + R_2}}\,(\xi_2 - \xi_1)^{3/2}\,\theta(\xi_2 - \xi_1)\,. \tag{35}$$

Here, θ is the Heaviside function, and E is the effective modulus dependent on the Young moduli of the materials constituting the spheres and their Poisson coefficients. When the displacement difference $(\xi_2 - \xi_1)$ has a negative value, the spheres are repulsed undistorted and F is zero. When the same difference is positive, force F depends on it as $(\xi_2 - \xi_1)^{3/2}$. Evidently, when the system of two spheres vibrates under the action of a periodic external force, the nonlinearity will be essential only if the contact area between the two bodies changes substantially. The nonlinearity decreases if the spheres are pressed against each other by a large static force. In the case of weak squeezing, stretching forces may break the contact; then, granules collide in the compression phase. Such

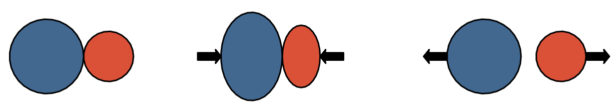

Figure 5. Nonlinear Hertz contact.

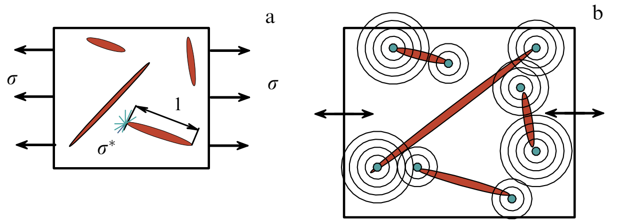

Figure 6. (a) The stress applied near the sharp tip of a crack is enhanced $K \gg 1$ times. (b) The crack tips emit harmonics and combination frequencies of the incident wave spectrum.

a mechanism is referred to as 'clapping' nonlinearity. The model of a system in which compressive and stretching strains are described by the linear Hooke law with distinct elastic moduli is called 'bimodular'; evidently, a system with 'clapping' contacts is a specific case of bimodular systems lacking in elastic resistance to stretching.

The nonlinear mechanisms similar to the Hertz contact mechanism described in the foregoing paragraphs are used in the dynamic description of granulated media (see Ref. [38]), contact between rough surfaces [22], and some other systems.

One more important example of media characterized by large structural nonlinearity is provided by a cracked medium (Fig. 6). It is known that the stress σ applied to a specimen of such a medium peaks at the tip of a sharp crack $(\sigma^* = K\sigma)$ where it is enhanced by $K = 1 + 2\sqrt{l/2r_0}$ times, where l is the crack length, and r_0 is the radius of curvature at the apex of the cut (see, for instance, Ref. [39]). When $r_0 \to 0$, the enhancement comes after $K \to \infty$. Large stresses exerting near the sharp tip of a crack cause plastic strain of the adjacent medium, while r_0 acquires a certain finite value.

Let an alternating stress be applied to a solid sample with internal cracks (Fig. 6a), say, through irradiation with a wave at frequency ω or two waves at frequencies ω, Ω. The homogeneous volume undergoes linear strain, but crack tips generate the second harmonic 2ω or combination frequencies $\omega + \Omega$ and $\omega - \Omega$ (Fig. 6b). The magnitude of the nonlinear response must increase as the number of cracks increases.

The influence of structural defects on concrete strain nonlinearity was observed in the course of ultrasonic and tensometric measurements [40–42]. It was found that water-saturated specimens exhibited pseudoelastic properties, and their nonlinearity enhanced upon evaporation of moisture (crack drying). Also, the frequency dependence of nonlinear effects and the development of hysteretic phenomena were revealed.

Robsman [43, 44] received direct confirmation of the enhancement of medium nonlinearity with an increase in the number of cracks (Fig. 7). An increasing static load was applied to a concrete beam on a test-stand as long as it took to break the structure. With increasing load, the number of cracks also increased, as well as the structural nonlinearity of the medium. Nonlinear wave interactions were enhanced even though the beam length (6 m) and the level of the initial signal remained unaltered. By way of example, Fig. 7 illustrates the coupling between the narrow line of the acoustic signal and the shock-induced broad noiselike spectrum (cf. Fig. 1a). The processes of generating higher harmonics and the appearance of wide 'pedestals' in each spectral line were most pronounced under large loads. The formation of new cracks gave rise to acoustic emission signals that were also involved in interactions. The spectrum

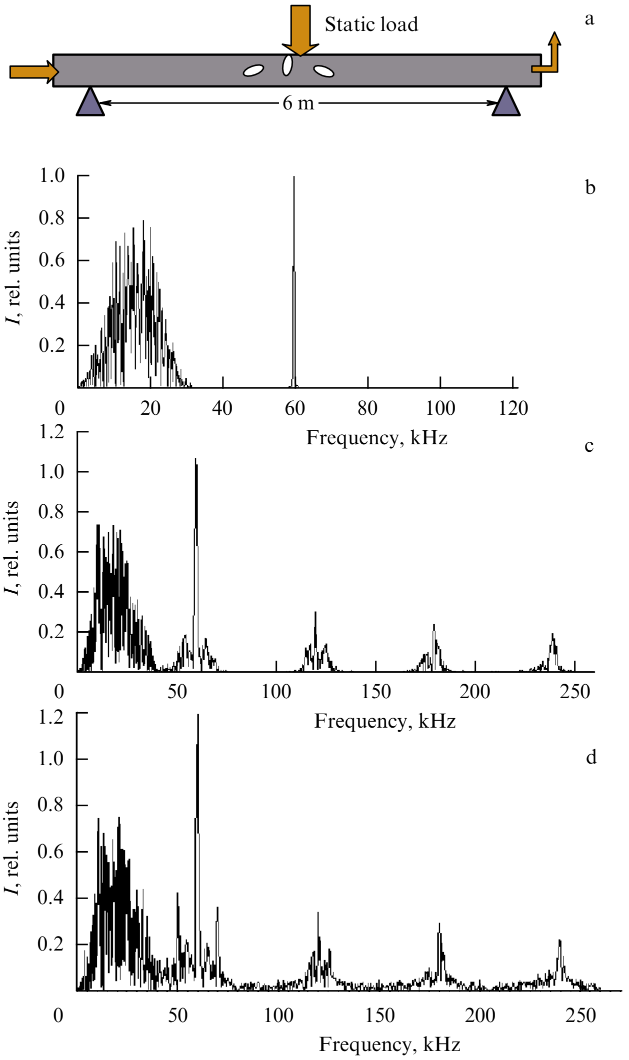

Figure 7. Nonlinear interactions of broadband noise and a monochromatic wave in a reinforced concrete beam (a) at different stages of crack formation: (b) in the absence of cracks, (c) with the appearance of single isolated microscopic cracks, and (d) during the development of a system of coupled cracks before a sudden fracture of the beam. I — output signal intensity.

became very complex just before the abrupt destruction of the specimen, with the continuous spectral component (white noise) being especially noticeable.

Naturally, the formation of a network of cracks leads to a decrease in material strength. Therefore, the enhancement of nonlinear effects in a defective medium may serve as a criterion of strength loss.

Many recent publications have been concerned with nonlinear acoustics of media with hereditary properties (including hysteretic ones). However, these works have thus far been largely dissociated from the previous many-year studies on hereditary media mechanics, initiated long ago by Boltzmann (1876), Rayleigh (1887), and Volterra (1913). The authors of these works prefer the term 'constitutive equations' to the former term 'equations of state' containing physical nonlinearity.

It was Volterra who constructed the nonlinear theory of hereditary elasticity using the Frechét representation for the functional in the form of multiple integral series generalizing the Taylor series. For a one-dimensional case, the Volterra–Frechét expansion in the scalar variant has the form

$$\sigma(t) = \int_{-\infty}^{t} G_1(t-\tau)\,\mathrm{d}e(\tau) + \int_{-\infty}^{t}\int_{-\infty}^{t} G_2(t-\tau_1, t-\tau_2)\,\mathrm{d}e(\tau_1)\,\mathrm{d}e(\tau_2) + \ldots, \tag{36}$$

$$e(t) = \int_{-\infty}^{t} J_1(t-\tau)\,\mathrm{d}\sigma(\tau) + \int_{-\infty}^{t}\int_{-\infty}^{t} J_2(t-\tau_1, t-\tau_2)\,\mathrm{d}\sigma(\tau_1)\,\mathrm{d}\sigma(\tau_2) + \ldots,$$

where σ, e are the stress and the strain, and G_n, J_n are the relaxation and creep functions, respectively [45]. Sometimes, model expansions are utilized, e.g., the Rabotnov equation

$$\varphi\big[e(t)\big] = \sigma(t) + \int_{-\infty}^{t} K(t-\tau)\,\sigma(\tau)\,\mathrm{d}\tau \tag{37}$$

or the Linderman–Rozovsky equation

$$e(t) = \psi\big[\sigma(t)\big] + \int_{-\infty}^{t} K(t-\tau)\,\chi\big[\sigma(t)\big]\,\mathrm{d}\tau\,, \tag{38}$$

where $\varphi(e)$, $\psi(\sigma)$ are certain functions; here, functional series (36) are assumed to be partly summed. In mechanics, these functions, as well as kernels in integrands entering Eqn (36), are selected based on a large body of experimental data for each particular material [45]. There are very fewer experimental data in acoustics, with its wider frequency range and considerably more complicated kernel (and spectrum) structure. Such data are available, in principle, by nonlinear spectroscopy, in analogy with optics (see, for instance, Ref. [46]), but we are unaware of any such measurements and of the developments in this field at large. In acoustics, the term 'nonlinear spectroscopy' is used in quite a different sense; for example, the term 'nonlinear resonance spectroscopy' is taken to mean a simple measurement of the amplitude-dependent frequency of resonator oscillations [47].

Theories like the Volterra theory are concerned with retarded processes that are reversible in the sense that instantaneous strain curves (in the stress–strain dependence) coincide for loading and unloading. The situation may be different in hysteretic media. For example, nonlinearity in metals is associated with the cumulation of essentially irreversible plastic deformation and the unloading law approximates a linear one. In materials characterized by destructive pseudoelasticity (e.g., reinforced plastics with stress concentrated about fibre bends, cracks), unloading results in the 'closure' of some cracks and the unloading graph approaches the origin of coordinates: $\sigma = e = 0$ [45]. Crack 'healing' in the process of deformation was observed in concrete. Recently, the phenomenon of the creation and annihilation of a defect was detected in metals as manifested by the generation of higher harmonics [48]. A model of the stress–strain dependence in the form of the Rayleigh hysteresislike dependence is convenient in describing cyclic processes. Such a hysteresis loop in Fig. 8a is defined by the following formulas (for sections A′B′A, ABA′)

$$\sigma = (E + be_{\mathrm{m}})e + \frac{b}{2}(e^2 - e_{\mathrm{m}}^2)\,,$$

$$\sigma = (E + be_{\mathrm{m}})e - \frac{b}{2}(e^2 - e_{\mathrm{m}}^2)\,,$$

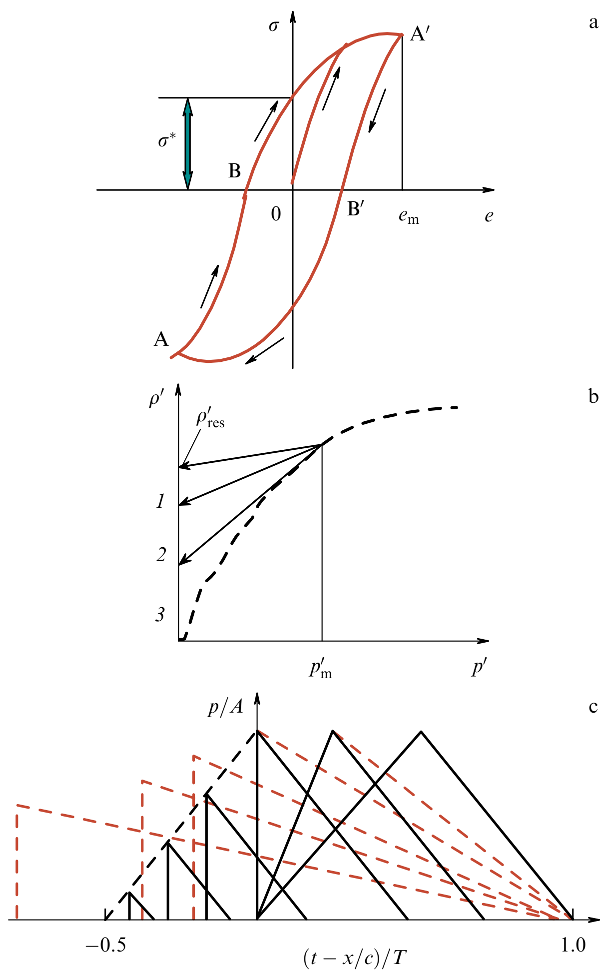

Figure 8. (a) Rayleigh hysteresis. (b) The process of wave-induced medium densification: loading follows the dashed curve, unloading — straight lines *1–3*. (c) The profile distortion of the unipolar pulse as it travels in a hysteretic medium (solid curves) and in an ordinary nonlinear medium (dashed curves).

and $\sigma = Ee - be^2$ (section OA′). Residual stresses and hysteresis loss (per cycle) are given by the following expressions

$$\sigma^* = \frac{b}{2}\, e_m^2\,, \qquad W = \oint e\,d\sigma = \frac{4}{3}\, e_m^3\,.$$

However, this model holds only for quasistationary processes: it is clear that in the case of quick changes in the applied acoustic pressure the internal restructuring of the medium falls behind and the internal processes get 'frozen' whatsoever at very high frequencies. Hysteresis loss determined by the loop area in Fig. 8a must decrease with increasing frequency. On the whole, the picture is reminiscent of the one described by the Mandel'shtam–Leontovich relaxation theory [7]. In this theory, however, a linear internal parameter (concentration of one of the chemically reactive components, vibrationally excited molecules, etc.) undergoes relaxation, approximating an equilibrium value with its own characteristic time T; this results in the emergence of 'linear memory' in the dependence of medium density perturbation on acoustic pressure [2]:

$$\rho' = \frac{p}{c^2} - \frac{\varepsilon}{c^4\rho}\, p^2 + \frac{m}{c^2\rho T}\int_{-\infty}^{t} \frac{\partial p(x,t')}{\partial t'} \exp\left(-\frac{t-t'}{T}\right) dt'\,. \qquad (39)$$

Despite additional loss ('second viscosity' [7]) introduced by internal motion, the response is reversible and, the wave having passed, the medium returns to equilibrium. In contrast, the removal of the loading in hysteretic media gives rise to a 'nonlinear memory' — that is, to irreversible deformations and residual stresses.

The authors of Ref. [49] described a soil-like medium compacted under a one-time loading (Fig. 8b), in which the unloading process may follow different paths, depending on its rate. The straight line *1* in Fig. 8b corresponds to a slow process, with residual strains attaining a maximum. In a rapid cycle, the straight line *3* is close to the loading curve. Here, as distinct from formula (39), the internal dynamics is described by the nonlinear integral term:

$$\rho' = \frac{p}{c^2} - \frac{\varepsilon}{c^4\rho}\, p^2 + \frac{\varepsilon}{c^4\rho}\,\frac{1}{T}\int_{t_m}^{t} \left[p(x,t') - p_m(x)\right]^2 \exp\left(-\frac{t-t'}{T}\right) dt'\,. \qquad (40)$$

Evolution type wave equations for these cases look different. For constitutive equation (39), the wave equation has the form [2]

$$\left(\frac{\partial}{\partial\tau} + \frac{1}{T}\right)\left(\frac{\partial p}{\partial x} - \frac{\varepsilon}{c^3\rho}\, p\, \frac{\partial p}{\partial\tau}\right) = \frac{m}{2c}\,\frac{\partial^2 p}{\partial\tau^2}\,;$$

for the case described by formula (40), it is written down [49] as

$$\left(\frac{\partial}{\partial\tau} + \frac{1}{T}\right)\left(\frac{\partial p}{\partial x} - \frac{\varepsilon}{c^3\rho}\, p\, \frac{\partial p}{\partial\tau}\right) = -\frac{\varepsilon}{2c^3\rho T}\,\frac{\partial}{\partial\tau}\left(p - p_m(x)\right)^2.$$

Figure 8c illustrates the process of transformation of a unipolar pulse in a usual nonlinear medium and in a medium with residual deformations. Some essential differences are obvious: (1) the pulse area is constant in the usual medium and decreases as the pulse propagates in the irreversibly deformable medium; (2) the speed of the trailing edge of a pulse is higher than that of the leading edge because the former spreads through the medium compacted by the latter; (3) the edges draw close together and thereby cause the pulse to 'collapse', and (4) in the usual medium, the pulse asymptotically decays as $x \to \infty$, while residual-strain loss results in its disappearance over a finite distance.

Analysis of direct and inverse wave problems appears to be of greatest interest in the area under consideration, and possibly for the purpose of nonlinear diagnostics. However, the majority of acoustic studies of hereditary media pertain to materials science and are descriptive in character. It follows from Fig. 8c that waves in such media behave differently than in the case of the ordinary stress–strain algebraic dependence. Nonlinear waves were the subject of in-depth studies [2] when their parameters were interrelated by 'relaxing' dependences (in the sense of the Mandel'shtam–Leontovich concept), but these results are insufficient to characterize hysteretic media (see the review of this problem in Refs [49–53]).

4. On nonlinear diagnostics

The basis for conventional acoustic diagnostics is the ability of sound waves to penetrate media opaque for other types of radiation. It is known that low-frequency waves can propa-

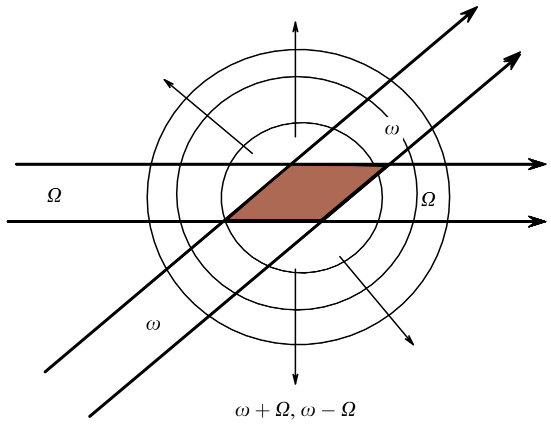

Figure 9. Sound-by-sound scattering and cross modulation in intense wave beams.

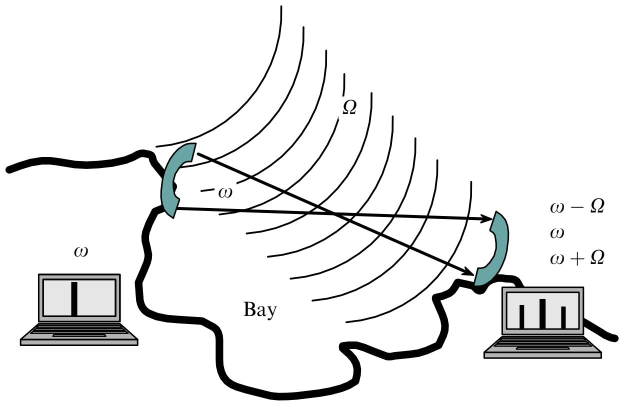

Figure 10. The principle of operation of a receiving 'parametric' antenna: the strong wave ω 'remembers' the parameters of a weak signal.

gate thousands of kilometers underwater or underground, while high-frequency waves are focused on any internal organ of the human body to produce its ultrasound image. That is why acoustic diagnostics finds such wide applications in geophysics, medicine, and industry. Linear methods allow selected objects to be examined by varying the frequency, phase, polarization, and traveling direction of waves. Nonlinear phenomena give rise to the dependence of the medium response on the signal amplitude (intensity). This introduces a 'new dimension' in many methods and schemes of acoustic diagnostics. In principle, any of the existing methods can be generalized and extended to a nonlinear case, with the number of such modifications being very large. Therefore, it appears appropriate to discuss here only those schemes in which nonlinearity has already opened up fresh interesting opportunities.

The ideas underlying nonlinear diagnostic and nondestructive testing techniques are well known. The growth of wave amplitudes leads to the violation of the superposition principle: strong waves intersect in time and space and the interaction between them is accompanied by the exchange of energy. In this process, each wave 'remembers' individual characteristics of its 'partners' and material characteristics of the medium (in the region where the interaction occurred). This information is 'delivered' to the receiver by the initial waves, which themselves undergo cross modulation, or by means of radiation emitted directly from the region of interaction in the form of new spectral components that were absent in the initial wave spectrum.

Figure 9 depicts the region of intersection of two wave beams with frequencies ω, Ω. This region can emit harmonics and combination frequency waves, the amplitudes of which depend on both the initial wave amplitudes and the parameters of the medium. Processing the signals provides information about linear and nonlinear properties of the medium in the interaction region. Moreover, each beam leaving this region undergoes modulation with the spectrum of another beam. These phenomena are underlain by the 'sound-by-sound scattering' effect [56] (see also Refs [57, 58] for more details). Devices that realize nonlinear 'storage' of the signal are exemplified by a 'parametric' sound receiver [10, 57] employed in hydroacoustics (Fig. 10). It uses as the receiving antenna a water column dozens or hundreds of meters in height in which an intense high-frequency beam ω is localized. Parametric devices utilizing the air to the same effect have begun to be increasingly applied for the remote diagnostics of certain objects [59].

Strictly speaking, the condition of synchronous (resonant) interaction between three waves at quadratic nonlinearity

$$\omega_3 = \omega_1 + \omega_2 \,, \qquad \mathbf{k}_3 = \mathbf{k}_1 + \mathbf{k}_2$$

in acoustic media with weak dispersion is fulfilled only for small beam intersection angles. Specifically, the directional characteristic of the receiver shown in Fig. 10 has a sharp peak in the direction of the emitted reference beam that makes up the 'immaterial' receiving antenna [10]. In experiments, however, it is also easy to measure effects of nonresonant scattering at any beam intersection angle. Hence the possibility of moving the intersection region in space to measure the distribution of medium characteristics. Also, it proved possible to realize an acoustic tomography scheme based on the use of colliding beams with a minimal length of synchronous wave interaction [60]. In this scheme, scanning the space was performed with the aid of delaying pulse signals; this technique ensured that the pulses met and interacted in different places.

The most complete information on the spatial distribution of the nonlinear parameter $\varepsilon(\mathbf{r})$ can be obtained using methods of diffraction reconstructive tomography. The simplest scheme has been described in Ref. [61]. Let a nonlinear region (e.g., a cloud of bubbles in water or in biological tissue or a network of cracks in a solid) be irradiated with waves ω_1, ω_2 directed along unit vectors $\mathbf{n}_1$, $\mathbf{n}_2$. The parameter measured is the difference frequency $\omega_3 = \omega_1 - \omega_2$ in the $\mathbf{n}_3$ direction. The solution of the nonlinear equation

$$\frac{\partial^2 p}{\partial t^2} - c^2 \Delta p = \frac{\varepsilon(\mathbf{r})}{c^2 \rho} \frac{\partial^2 p^2}{\partial t^2}$$

in the Born approximation for the amplitude of the difference signal in the far field takes the form

$$P_3 = \frac{\pi^2 \omega_3^2}{c^2 \rho} \frac{\exp\left(\mathrm{i}(\omega_3/c) r\right)}{r} P_1 P_2^* \tilde{\varepsilon}\left(\frac{\omega_3}{c}\,\mathbf{n}_3 - \frac{\omega_1}{c}\,\mathbf{n}_1 + \frac{\omega_2}{c}\,\mathbf{n}_2\right), \tag{41}$$

where $\tilde{\varepsilon}(\mathbf{k})$ is the Fourier transform of function $\varepsilon(\mathbf{r})$, and the origin of coordinates is inside the scatterer. For collinear probing waves, $\mathbf{n}_1 = \mathbf{n}_2$, the outer term in formula (41) becomes

$$\tilde{\varepsilon} = \tilde{\varepsilon}\left[\frac{\omega_3}{c}(\mathbf{n}_3 - \mathbf{n}_1)\right]. \qquad (42)$$

In other words, vectors $\mathbf{n}_3$, the ends of which are located on a sphere of unit radius, are possible to measure for each direction of irradiation. In this way, the values of the argument of the Fourier transform (42) on a sphere of radius ω_3/c are determined. By varying the difference frequency or using different combinations of the directions of irradiation and reception, it is possible to fill with measurement data the inside of the corresponding sphere in the **k**-space. After this, the $\varepsilon(\mathbf{r})$ distribution is reconstructed by numerical methods that realize the inverse Fourier transform.

The ability of a nonlinear wave to 'remember' the properties of the track is used for the diagnostics of tapered waveguides [62]. If function $S(x)$ describing cross section changes is unknown, it can be found by solving Eqn (7) for the second harmonic, represented in the form of the Fredholm integral equation

$$\frac{2c_0^3\rho_0}{\varepsilon\omega}\,\frac{P_2(x)}{P_0^2(x)} = \int_0^x \left[\frac{S(x)}{S(z)}\right]^{1/2} \exp\left[\frac{b\omega^2}{c_0^3\rho_0}(z-x)\right] \mathrm{d}z\,.$$

The channel profile can be reconstructed using the amplitude values of both harmonics measured at distance x and at different frequencies of the initial signal.

It was proposed in Ref. [63] to recruit another effect for channel profiling — that is, the phenomenon of self-reflection after the formation of shock fronts in the wave [2]. By varying the initial wave amplitude, it is possible to change the distance at which the shock-wave discontinuity occurs, this distance being also integrally dependent on the channel cross section. Measurement of the arrival time of the self-reflected signal [64], the forward front of which is delayed by time $2l_{\mathrm{NL}}/c_0$ (11) with respect to the probing pulse, makes it possible to form a data array for the solution of the inverse problem.

It follows from the above that the general approach to the reconstruction of the boundaries and the internal structure of nonlinear scatterers should be based on the methods for the solution of inverse problems realized in nonlinear acoustic tomography. However, even the simplest diagnostic technique by means of the generation of harmonics and combination frequencies is highly efficient, especially when the medium contains strongly nonlinear inclusions like bubbles or cracks. Actually, any analytical solution of a direct nonlinear problem includes parameters (nonlinear moduli, wave amplitudes, and geometric characteristics) that can be found through experiment by measuring the nonlinearly distorted wave field or its spectrum.

Let us consider some basically essential features of nonlinear diagnostics.

The dependence of the medium response on the probing wave amplitude (intensity) may be employed to reveal internal damages in a medium in the absence of *a priori* information about the influence of defects on the variation of the response. For example, if a batch of details is to be checked for quality by an ordinary (linear) method, an 'acoustic certificate' of an ideal (intact) item is needed. The degree of damage can be estimated by comparing the responses of the defective and intact articles. Conversely, no comparison is needed if the defect constitutes a nonlinear scatterer. Suffice it to perform a series of measurements at different intensities of sound excitation inside an article of interest (Fig. 11). If the time response stops growing linearly with increasing excitation amplitude (in this case, the response acquires new characteristics) or if its spectrum displays new components, these findings give reason to reject the article. The simplest diagnostic method based on exciting the shock-induced sound has long been used to check the integrity of the pairs of wheels for railway cars; the quality of cut glassware and porcelain objects is evaluated on the same principle from the clatter produced by tapping. It should be noted that a shock may induce a pulse signal with pronounced nonlinear behavior, which is able to interact with a rather weak wave that lacks nonlinearity in itself. Today, such interactions are frequently used for diagnostic purposes (see, for instance, Fig. 7).

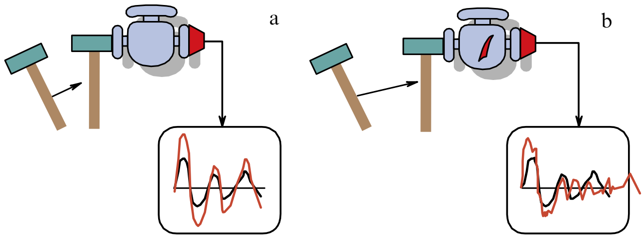

Figure 11. Response of an intact article is enhanced linearly with increasing impact force (a); the time and spectral responses of a defective article display new features (b).

The difference between the linear and nonlinear responses found application in many measuring schemes. For example, the 'inverted pulse method' is used in medicine. With this technique, a volume of interest is first probed with a pulsed signal $p_1(t)$ followed by an identical one but with pressure inversion, $p_2(t) = -p_1(t)$. The scattered signals are recorded by a receiver and the readings are used to deduce the difference. The linear scatterer produces a zero difference, while the presence of nonlinearity results in a nonzero difference. The advantages of this approach also include the possibility of focusing the probing signals into a predetermined space region thereby increasing the nonlinear response by K^2 times (where K is the amplification coefficient of the probing signals at the focus). Another advantage is the possibility of detuning from disturbances created by reflections from the surface (skin) and bulk inhomogeneities.

Moreover, some medical diagnostic tools take advantage of a nonlinear method by which to control the ultrasound energy absorption in order to raise the degree of localization of biological tissue heating or excite radiation forces in these tissues. It is known that excessive absorption of intense waves may be substantially higher than the usual dissipative losses [1 – 3]; this phenomenon is especially apparent in the case of strongly distorted waves with shock fronts [8]. When the intensity of ultrasound amounts to several kilowatts per 1 cm^2 as in the focal regions of modern medical devices, the nonlinear absorption coefficient is one order of magnitude higher than the linear one [65 – 68]. Evidently, the task is to transmit the acoustic energy to a given region of the medium with minimal losses and to ensure its complete absorption there. This goal is achieved by a preliminary distortion of the wave being emitted, such that it ensures the formation of shock fronts in the immediate focal region during nonlinear diffractional evolution of the wave profile. The shape of the

Figure 12. Water jet formation under the effect of radiation pressure. (Photograph — by courtesy of O A Sapozhnikov).

thus evolving wave is calculated from the solution of the nonlinear inverse problem [68].

The phenomenon of energy concentration at the focus is employed in acoustic hyperthermia (thermal destruction of malignant neoplasms), ultrasound hemostasis (arrest of internal bleeding by noninvasive vascular coagulation) [67], decomposition of intracellular structures in order to trigger an immune response to neoplasia [69], and other medical situations. We shall consider here only diagnostic tools making use of pulsed radiation forces being created inside the object under study by focused ultrasound. Radiation pressure, discovered by Rayleigh in 1902, is a strong effect much in excess of light pressure. Suffice it to say that ultrasound focused on the water surface may produce a jet about 10 cm in height (Fig. 12). Absorption of ultrasound or its reflection from inhomogeneities in the medium creates an eddy field of forces. The appearance of these forces is formally explained by the presence of nonlinear terms in the equations of hydrodynamics (1), (2) and the theory of elasticity (3), (4), when these equations are averaged over rapid oscillations [2]. Hence the formation of flows ('acoustic wind') in liquids, and stresses in biological tissues. When ultrasound is modulated with low frequencies, the alternating field of force far from the boundaries excites shear waves. These waves can be detected [70] and their speed of propagation used to evaluate shear elasticity that is highly responsive to pathological changes in the tissues [71]. In particular, it increases by 2 or 3 orders of magnitude in tumor tissue, whereas the variation of other parameters (medium density, velocity of sound) does not exceed several percent. Based on this fact, a new diagnostic tool (SWEI) was proposed (see Section 5).

Shear waves are susceptible to structural inhomogeneities responsible for large nonlinearities [24]. Therefore, the method of remote excitation of shear waves may be used to test construction materials in not easily accessible areas, for example, in the analysis of fatigue strength at the wing/fuselage joints of aircraft. This problem is currently discussed in connection with the realization of new diagnostic schemes.

The advent of acoustic resonators has opened up new opportunities for the measurement of nonlinear medium parameters. Usual values of the Q factor for these devices are 10^2-10^4. The oscillation amplitude in the cavity of a resonator is that much higher than the vibration amplitude of its border. It implies the possibility of using in experiments substantially less powerful sources than in measurements performed with the use of running waves. Record-breaking values of the quality factor (10^8-10^9) were obtained by Braginsky's group [72] when they developed detectors of gravitational waves. The possibilities for the improvement of the quality factor with regard to strong manifestations of nonlinearity were analyzed in Ref. [73]. Measurements of nonlinear parameters of various media in acoustic resonators were initiated by Zarembo and co-workers in the 1960s [1]. In a later work, Zarembo et al. [40] discussed evaluation of concrete's strength based on acoustic data. The authors demonstrated that ultimate compression and tensile strengths were governed simultaneously by quadratic and cubic nonlinearity coefficients. The cubic nonlinearity was measured from the downward shift of resonator eigenfrequency; when the acoustic strain amplitude increased from 10^{-7} to 7×10^{-6}, the eigenfrequency of a concrete block decreased by $\Delta f = 5\times10^{-3} f_0$ (at a strain of 7×10^{-6}) from the initial value $f_0 = 6.033$ kHz. Strength estimates deduced from nonlinear parameters were in excellent agreement with the previously known data. At present, measurements in resonators are being carried out in other laboratories (see, for instance, Refs [13, 47]).

It is worthwhile mentioning the recently developed methods based on time reversal of weak waves for the formation of intense and sharply focused signals [47]. First, a weak pulse from a small source is fed into a vessel (tube) where it becomes considerably protracted as a result of multiple reflections. The enduring signal is received, recorded, and reversed in time; thereafter, it is amplified and sent in the opposite direction. On the way back, the pulse again undergoes multiple reflections, becomes compressed in time, and turns into a short intense pulse focused onto the same small area from which the initial weak pulse originated.

Nonlinear diagnostics also make use of front-reversed signals [74]. This issue was discussed in another report presented at the session of the RAS Physical Sciences Division [75].

5. Certain applications

Recent years have given rise to the publication of a considerable number of works dealing with the nonlinearities of inhomogeneous media, various materials, industrial articles, building constructions, and geological structures, including methods of their nonlinear diagnostics. A group of scientists from almost ten European countries known as NATEMIS was set up and meets once or twice a year at workshops and has recently organized a series of aviation diagnostic studies. Similar works carried out in the USA are concerned with geological surveys, analysis of nuclear energetics safety, and various branches of industry. Increasing interest in these issues is stimulated not only by their obvious practical implications but also by their bearing on some unresolved fundamental problems of nonlinear physics and materials science. In what follows, we discuss examples of the diagnostic application of certain nonlinear phenomena.

The detection of single gas bubbles and their accumulations in liquids, dwelt on in Section 3, has found applications in medicine, unexpected for Russian specialists. Specifically, it provided a basis for producing contrast agents, such as Albunex, to be used to visualize blood flow and in other areas of medical diagnostics. The extent of this work is illustrated by the fact that American and European companies have

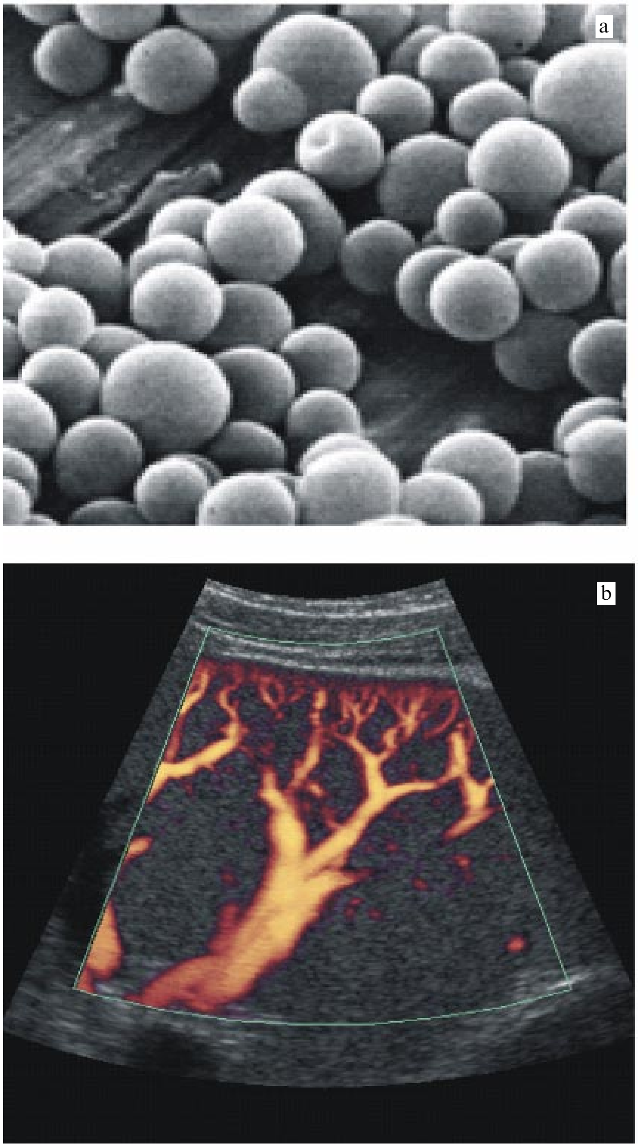

Figure 13. (a) Bubbles in an acoustically contrasted preparation, and (b) a vascular bed segment visualized using this agent. (Photographs — by courtesy of V A Khokhlova).

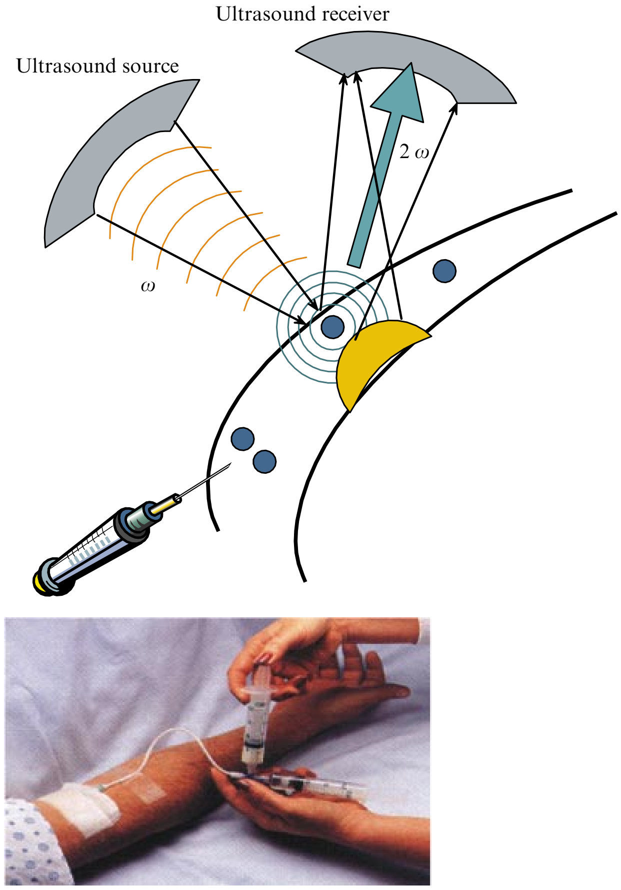

Figure 14. Diagram and photo illustrating the use of bubble-containing preparations for blood flow visualization.

already invested hundreds of millions of dollars in the development and clinical testing of these agents. Albunex constitutes a stable suspension of micrometer-sized bubbles each enclosed by a biologically inert membrane (Fig. 13). The bubbles are injected intravascularly and their transport with the blood flow is registered from the usual sound scattering or based on the second harmonic and combination frequency (Fig. 14). Marked local nonlinearity in the absence of disturbances from linear scatterers on higher harmonics makes it possible to keep watch on isolated bubbles and small groups thereof or follow the travel of the bubble cloud front; also, a vascular bed segment can be visualized as a whole.

A similar problem was successfully resolved as applied to the detection of bulk defects (cracks) in manufactured solid articles. Large nonlinearity of the cracks allows for their visualization on higher harmonics. By way of example, Fig. 15a shows a plate surface undergoing vibrations at a frequency of 20 kHz; the relief of surface displacements was visualized with a laser vibrometer. At this frequency, the signal from the crack is invisible against the background of the surface signal that (in the case under consideration) acts as noise. In contrast, the same signal recorded at higher harmonic frequencies reveals a well-apparent crack (Fig. 15b) because the harmonic (in this experiment, the seventh one) results, first and foremost, from crack vibrations and surface displacements do not interfere with the desired signal.

A most interesting nonlinear dynamics of an isolated defect in a solid was observed in experiment [48] (see Fig. 16). The authors excited different vibrational modes of a metal disk and recorded the distribution of surface acoustic displacements by a Polytec vibrometer. The displacement pattern of one of the modes is depicted in Fig. 16a. The mode spectrum was not equidistant, and a few first harmonics of the principal mode did not match the higher mode frequencies. For this reason, the excitation of the disk at the second–fourth harmonics produced only small surface displacements but fairly well revealed vibrations of the internal defect, most likely a crack (Fig. 16b). The local anomaly disappeared after the prolonged exposure of the defect to large-amplitude vibrations, probably due to 'self-healing' of the crack. The signal was observable when the displacements at the first harmonic reached 10^{-5} m; it existed in a narrow dynamic range of some 10^{-6} m. The maximum displacements on the second, third, and fourth harmonics were estimated at 2×10^{-7}, 1.2×10^{-7}, and 0.2×10^{-7} m.

The shear wave elasticity imaging (SWEI) technique proposed by Sarvazyan [71] is based on the remote excitation

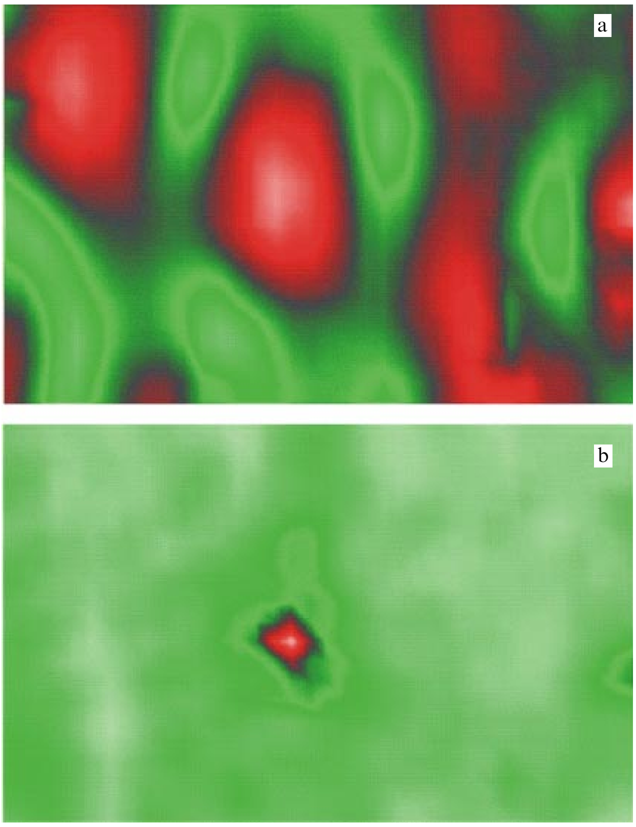

Figure 15. (a) Plate surface area vibrating at 20 kHz, and (b) a local subsurface defect visualized on the seventh harmonic (140 kHz). (Images — by courtesy of I Yu Solodov).

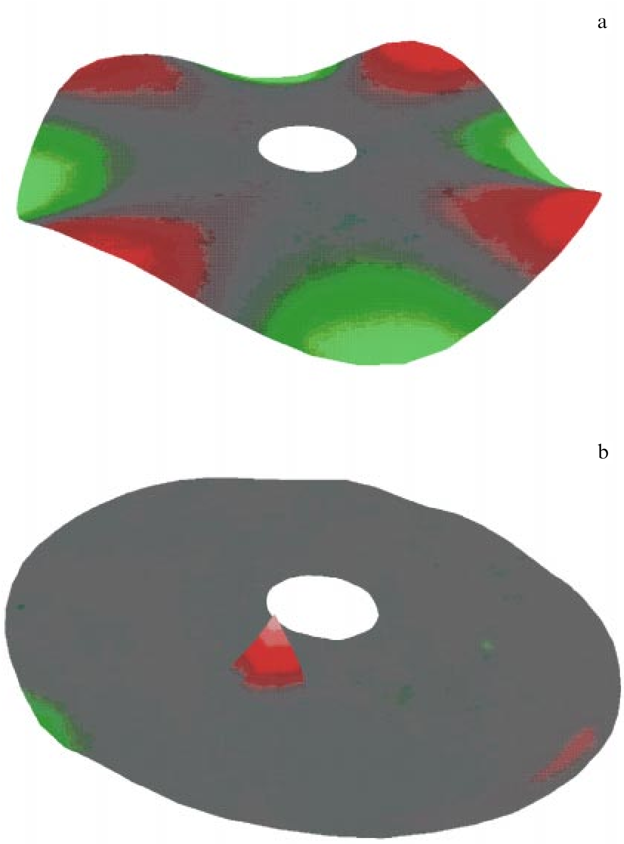

Figure 16. (a) Vibrational eigenmode of a metal disk, and (b) vibrations of the defect at the third harmonic of the principal mode. Results provided by A I Korobov and M Yu Izosimova. The electronic version of their paper available at http://www.ufn.ru shows these vibrations in dynamics.

of shear waves inside an object by pulsed radiation pressure created by an intense modulated and focused ultrasound beam. The idea behind the method is to utilize ultrasound, like surgeon's fingers, to 'palpate' internal organs and tissues of the human body (see Fig. 12). The area in which radiation forces are concentrated extending along the axis of the focal region [66], it emits a cylindrical shear wave that diverges from the axis (Fig. 17). This wave propagates with a low speed compared with the speed of sound; it may vary in the range from several to hundreds of meters per second, depending on the tissue properties. The speed was measured by an optical method (in a transparent phantom [70]) and also by nuclear magnetic resonance or from the Doppler frequency shift of

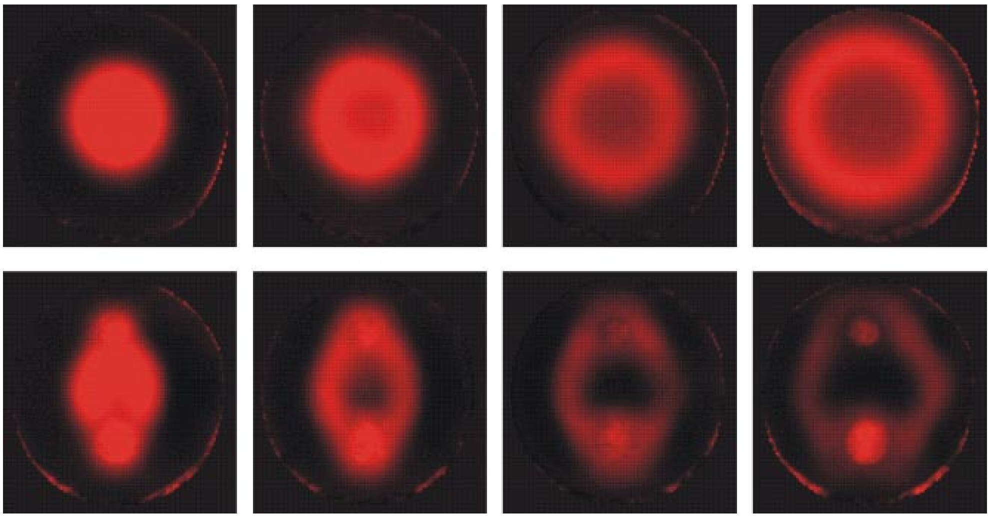

Figure 17. Consecutive positions of the shear wave front in a homogeneous phantom of biological tissue (top row). Inhomogeneous medium with two inclusions simulating a tumor (lower row). (Photographs — by courtesy of A P Sarvazyan). The electronic version of their paper available at http://www.ufn.ru shows the process of visualization in dynamics.

the probing ultrasound beam [71]. With this approach, it is possible to measure the parameter (shear elasticity) most vulnerable to pathological changes. It is worth noting that the term local compaction used to describe a palpable tumor is incorrect. The inhomogeneity that is subjectively perceived as compaction is actually a region of enhanced shear elasticity.

At present, Artannlabs [71] is developing a modification of SWEI for the diagnosis of bone and joint disorders. In this case, ultrasound penetrates soft tissues and produces radiation pressure on the bone, exciting various acoustic modes. The propagation speed contains information about deficient calcium content, and the analysis of the output signal spectrum provides data on other abnormalities.

Evidently, the idea of employing radiation pressure is equally promising for diagnostics of complex constructions because the respective method may be used for the contactless excitation of vibrations of an isolated element inside a construction and for analyzing its response.

Noteworthy among the achievements in the field of nonlinear acoustic diagnostics reached in this country are the results of its application in the building industry. These studies date back to the late 1980s. A group headed by V A Robsman at the Institute of Transport Construction (TsNIIS) was participating in the construction of the Sevan – Arpa tunnel in Armenia, when a devastating earthquake levelled the city of Spitak, caused severe damage, and killed thousands of people. The researchers were asked to assess the state of damaged buildings and to enable decision-makers to choose which ones to reconstruct and which to demolish for safety reasons. Ultrasound-raying of key construction elements (beams, load-bearing walls, span panels, etc.) demonstrated that the greater the damage, the stronger the distortion of the acoustic spectrum. The empirical criteria were later explained based on the results of experimental (see Fig. 7) and theoretical [43, 44] studies; since then, the reliability of 'nonlinear' forecasts has substantially improved.

The diagnostic methods developed in this country have been successfully employed in the construction of the Moscow Third Ring Road (see, for instance, Ref. [49]), reconstruction and restoration of historical architectural monuments (Fig. 18), building of subway lines, inspection of power facilities with a view to strengthening their structures and improving seismic resistance, and diagnostics of defects in the piers of large bridges and other long-span structures (over 30 in number) for assessing their real carrying capacity and the elaboration of projects of their reconstruction.

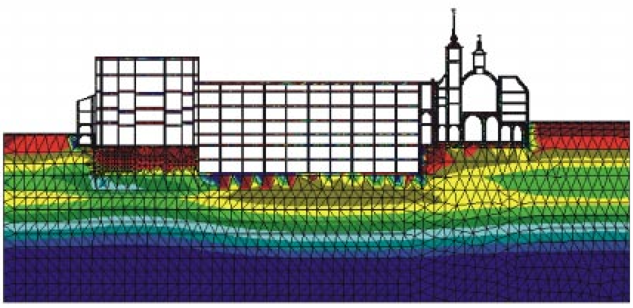

Figure 18. Illustration to a computer model for the calculation of force interactions between a new building and an old church in Moscow. Characteristics of the church building were obtained by acoustic diagnostic techniques. The construction project was not implemented. (Drawing — by courtesy of V A Robsman).

6. Atypical nonlinear phenomena in structurally inhomogeneous media

Structurally inhomogeneous media are of interest due to certain nonlinear phenomena manifested in them, besides the giant nonlinearity that accounts for the high sensitivity of nonlinear measuring methods.

One such phenomenon is the presence of a 'dominant' frequency in such media as wet sand, clay, and cracked rocks. The 'dominant' output signal is recorded in these media regardless of the frequency at which their vibrations are excited, while other spectral components, including the initial frequency, remain weak [76 – 79]. Characteristic values of the dominant frequency for gravel are 8 – 10 Hz, sea sand 25 Hz, clay 40 Hz, and eroded granite 100 Hz [77, 78]. Interestingly, the action of vibrations with a dominant frequency of 12 Hz on an irrigated oil-bearing stratum resulted in a two-fold increase in the share of oil in the total debit [80]. Dominant frequencies appear by virtue of the internal resonant properties of fragmented soils and rocks and their strong nonlinearity responsible for the vibrational energy transfer to these frequencies.

By 'ordinary' nonlinear phenomena are meant such processes as the generation of higher harmonics, subharmonics, and combination frequencies. In this context, direct generation of a very high (e.g., the hundredth) harmonic without previous generation of a cascade of lower harmonics looks unusual. Similarly, the generation of a low-frequency spectrum with characteristic frequencies considerably lower than the pump frequency looks, at first sight, rather exotic. Nevertheless, these processes do occur and have a rather simple explanation.

Let us consider an ensemble of granules imbedded in a liquid. The structure of such a system is strongly nonlinear in itself due to boundary contacts. The presence of an oscillating liquid gives rise to an additional inertial nonlinearity caused by the accelerated particle motion [38]. The streamlining of particles by the liquid generates attractive forces between them, while deformation of colliding granules results in their Hertzian repulsion (35) (see Fig. 5). Here, large spatial force gradients are due to the marked nonuniformity of the mass distribution. The linear eigenfrequency of vibrations of an elementary oscillator in such a medium is given by

$$f_{\text{lin}} = \frac{1}{2\pi}\sqrt{\frac{3a}{2}}\left(E^2 F_0 \frac{R_1 R_2}{R_1 + R_2}\right)^{1/6}, \tag{43}$$

where a is a coefficient dependent on the volumes and densities of two neighboring spherically shaped particles, F_0 is the static pressing force, and the remaining notations are the same as in formula (35). However, the nonlinear frequency for the vibration amplitudes A close to the granule diameter, viz.

$$f_{\text{nonl}} = \frac{a^{1/2} F_0^{5/6}}{2AE^{1/3}} \frac{R_1 + R_2}{R_1 R_2}, \tag{44}$$

turns out to be 2 – 3 orders of magnitude smaller. An acoustic wave running through the liquid makes granules attract one

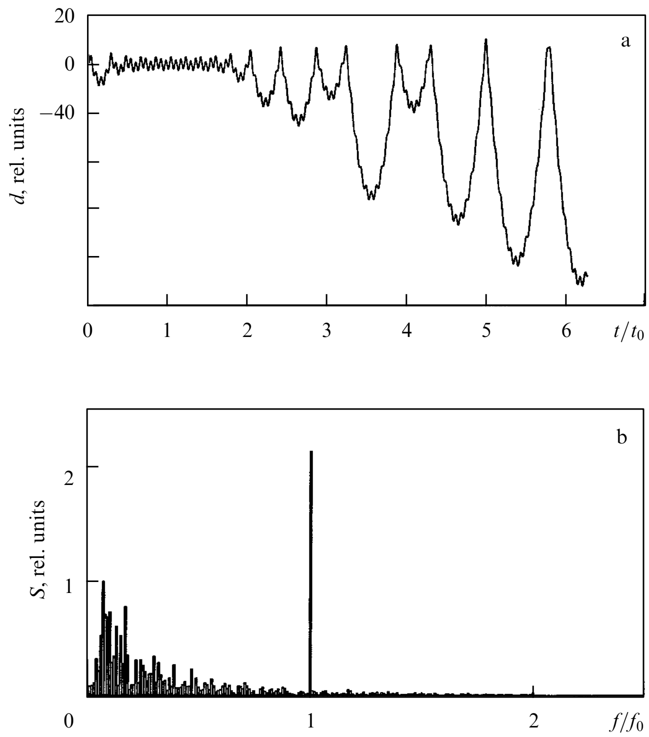

Figure 19. (a) Time dependence of the distance between the centers d of neighboring granules. (b) Stationary spectrum S of these vibrations.

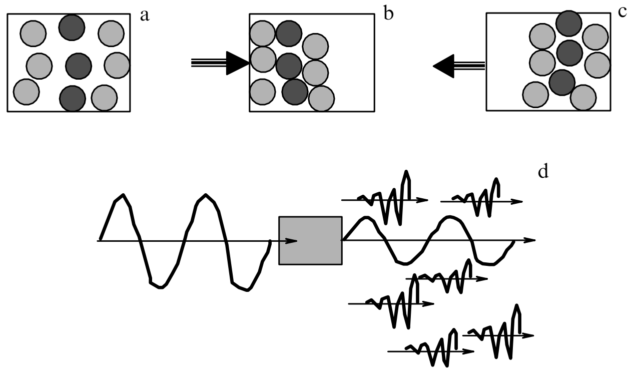

Figure 20. Schematic representation of structural changes in a volume with weakly consolidated units: (a) system at rest; (b) rigid boundary of the volume is accelerated by a wave to the right; (c) a change in wave polarity causes the repacking of units, and (d) input and output signals in the structure depicted in figures a – c.

another, collide, and then slightly diverge to move almost freely within the medium. After each new collision, the granules turn out to be farther and farther apart. The relative velocities of neighboring granules at the moment of collision being random, the resulting picture is that of random vibrations (Fig. 19a). The mean vibration amplitude grows with time, and the spectrum shifts to the low-frequency region (Fig. 19b).

Such behavior of granules has many analogies. A similar picture is observed in the field of gravity force when a ball elastically rebounds off a horizontal plate oscillating along the normal to its surface. The ball dropping on the plate at random instants of time after the onset of vibrations jumps up higher and higher after each fall until the energy receipts and losses achieve equilibrium. This process was first described in the 1920s by N N Andreev [81], a pioneer in acoustic research in this country; hence its name 'Andreev's hammer' (see Refs [82, 83]). Stochastic speed-up of the particles (Fermi acceleration) is invoked for explaining many phenomena; in the simplest model, this process is described by the Ulam point transformation [84].

Let us consider now the generation of high-frequency spectra. Let a confined volume of a medium contain discontinuities and look like a set of loosely pressed or free blocks. An example is a geological structure of the so-called 'weakly consolidated units' (Fig. 20a). An acoustic wave with a wavelength larger than the size of an inhomogeneity, propagating through such a medium, causes the appearance of quasistatic strains due to the inertia of separate structural units. Let periodic pressure changes accelerate the rigid boundary of the volume of interest in the positive direction (Fig. 20b); during this process, the units are displaced and packed. A change in the acceleration sign results in repacking (Fig. 20c). Each collision of units (blocks) with one another and with the boundaries of the consolidated medium induces a high-frequency pulse with a frequency on the order of the inverse time of sound passage through the block. Another characteristic frequency is determined by the number of collisions per period (i.e., the number of blocks in the bulk). Because the acoustic spectrum of each such impact lies much higher than the incident wave frequency, the structure presented in Fig. 20 generates a high-frequency noise acoustic field. The output spectrum contains, besides the initial low frequency, collision frequency harmonics and a set of eigenfrequencies ('ringing') of separate blocks (Fig. 20d).

A similar transformation of the acoustic spectrum takes place in a rattle, a Latin American musical instrument also known as a maraca. Shaking a hollow vessel containing granules produces vibrations with frequencies on the order of 1 Hz that undergo transformation into the audio-frequency band. Certainly, separate units of a geological structure travel distances much smaller than their sizes.

The existence of mechanisms that transfer the vibrational energy to the low-frequency (see Fig. 19) and high-frequency (Fig. 20d) spectral regions means that the signal being received after it passes through a real structurally inhomogeneous medium carries information not only about its source but even more so about its track. Marked spectral changes were observed when an earthquake-induced seismic wave spread across a tectonic break [77]. This means that the signals from distant earthquakes may be used for the purpose of nonlinear diagnostics of localized geological structures by measuring incident and scattered signals [85].

In conclusion, it should be noted that the number of publications on giant nonlinearities and nonlinear diagnostics continues to grow in the Russian and foreign scientific literature. To mention but a few, in addition to the works cited in this review, there are some recent ones devoted to nonlinear diagnostics of metals [86], granulated media [87], gas bubbles in biological tissues [88], etc. A supplementary issue of the *Akusticheskii Zhurnal* (*Acoustical Physics*) was out in 2005 with articles on the problems related to acoustics and geophysics. Large amounts of information can be found in the abstracts and proceedings of numerous conferences held in the past 2 – 3 years. Reports by my colleagues presented in this issue of *Physics – Uspekhi* further illustrate the current situation in the field of keen interest.

References

1. Zarembo L K, Krasil'nikov V A *Vvedenie v Nelineinuyu Akustiku* (Introduction to Nonlinear Acoustics) (Moscow: Nauka, 1966)
2. Rudenko O V, Soluyan S I *Teoreticheskie Osnovy Nelineinoi Akustiki* (Theoretical Foundations of Nonlinear Acoustics) (Moscow: Nauka, 1975) [Translated into English (New York: Consultants Bureau, 1977)]
3. Naugolnykh K A, Ostrovsky L A *Nelineinye Volnovye Protsessy v Akustike* (Nonlinear Wave Processes in Acoustics) (Moscow: Nauka, 1990) [Translated into English (New York: Cambridge Univ. Press, 1998)]
4. Landau L D, Lifshitz E M *Teoriya Uprugosti* (Theory of Elasticity) (Moscow: Nauka, 1987) [Translated into English (Oxford: Pergamon Press, 1986)]
5. Zarembo L K, Krasil'nikov V A *Usp. Fiz. Nauk* **102** 549 (1970) [*Sov. Phys. Usp.* **13** 778 (1971)]
6. Rudenko O V *Usp. Fiz. Nauk* **149** 413 (1986) [*Sov. Phys. Usp.* **29** 620 (1986)]
7. Landau L D, Lifshitz E M *Gidrodinamika* (Fluid Mechanics) (Moscow: Nauka, 1988) [Translated into English (Oxford: Pergamon Press, 1986)]
8. Rudenko O V *Usp. Fiz. Nauk* **165** 1011 (1995) [*Phys. Usp.* **38** 965 (1995)]
9. Rudenko O V, Robsman V A *Dokl. Ross. Akad. Nauk* **384** 755 (2002) [*Dokl. Phys.* **47** 443 (2002)]
10. Novikov B K, Rudenko O V, Timoshenko V I *Nelineinaya Gidroakustika* (Nonlinear Underwater Acoustics) (Leningrad: Sudostroenie, 1981) [Translated into English (New York: AIP, 1987)]
11. Guyer R A, Johnson P A *Phys. Today* **52** (4) 30 (1999)
12. Rudenko O V *Defektoskopiya* **29** (8) 24 (1993) [*Russ. J. Nondestructive Testing* **29** 583 (1993)]
13. Ostrovsky L A, Johnson P A *Riv. Nuovo Cimento* **24** (7) (2001)
14. Sarvazyan A P, Chalikian T V *Ultrasonics* **29** 119 (1991)
15. Chalikian T V et al. *J. Acoust. Soc. Am.* **91** 52 (1992)
16. Rudenko O V, in *Nelineinye Volny-2004* (Nonlinear Waves-2004) (Eds A V Gaponov-Grekhov, V I Nekorkin) (Nizhnii Novgorod: IPF RAN, 2005) p. 70
17. Rudenko O V *Akust. Zh.* **44** 823 (1998) [*Acoust. Phys.* **44** 717 (1998)]
18. Rudenko O V *Akust. Zh.* **45** 397 (1999) [*Acoust. Phys.* **45** 351 (1999)]
19. Rudenko O V, Shanin A V *Akust. Zh.* **46** 392 (2000) [*Acoust. Phys.* **46** 334 (2000)]
20. Rudenko O V, Khirnykh K L *Akust. Zh.* **36** 257 (1990) [*Sov. Phys. Acoust.* **36** 293 (1990)]
21. Severin F M, Solodov I Yu, Shkulanov Yu N *Vestn. Mosk. Univ. Ser. 3 Fiz. Astron.* **29** (4) 94 (1988) [*Moscow Univ. Phys. Bull.* **29** (4) 94 (1988)]
22. Rudenko O V, Chin A V *Akust. Zh.* **40** 688 (1994) [*Acoust. Phys.* **40** 593 (1994)]
23. Richardson T *Int. J. Eng. Sci.* **17** 73 (1979)
24. Zheng Y, Maev R G, Solodov I Yu *Can. J. Phys.* **77** 927 (1999)
25. Hedberg C M, Rudenko O V *J. Acoust. Soc. Am.* **110** 2340 (2001)
26. Ostroumov G A et al., in *Tr. 6 Mezhdunarodnogo Simpoziuma po Nelineinoi Akustike* (Proc. of the 6th Intern. Symp. on Nonlinear Acoustics) (Moscow: Izd. MGU, 1975) p. 209
27. Druzhinin G A, Mikhailov A A, Tokman A S *Akust. Zh.* **34** 176 (1988) [*Sov. Phys. Acoust.* **34** 99 (1988)]
28. Kobelev Yu A, Sutin A M *Akust. Zh.* **26** 860 (1980) [*Sov. Phys. Acoust.* **26** 485 (1980)]
29. Zamolin S et al. *Acoust. Lett.* **6** (2) 15 (1982)
30. Zabolotskaya E A, Soluyan S I *Akust. Zh.* **13** 296 (1967) [*Sov. Phys. Acoust.* **13** 276 (1967)]
31. Nakoryakov V E, Pokusaev B G, Shreiber I R *Volnovaya Dinamika Gazo- i Parozhidkostnykh Sred* (Wave Dynamics of Gas- and Vapor-Liquid Media) (Moscow: Energoatomizdat, 1990)
32. Lyakhov G M *Osnovy Dinamiki Vzryvnykh Voln v Gruntakh i Gornykh Porodakh* (Principles of Dynamics of Blast Waves in Grounds and Bed-Rocks) (Moscow: Nedra, 1974)
33. Mansfel'd A D, Reiman A M, in *Ul'trazvukovaya Diagnostika* (Ultrasound Diagnostics) (Ed.-in-Chief M T Grekhova) (Gor'kii: IPF USSR AN, 1983) p. 139
34. Ostrovskii L A, Sutin A M, in *Ul'trazvukovaya Diagnostika* (Ultrasound Diagnostics) (Ed.-in-Chief M T Grekhova) (Gor'kii: IPF USSR AN, 1983) p. 151
35. Isakovich M A *Obshchaya Akustika* (General Acoustics) (Moscow: Nauka, 1973)
36. Vinogradova M B, Rudenko O V, Sukhorukov A P *Teoriya Voln* (Wave Theory) 2nd ed. (Moscow: Nauka, 1990)
37. Brekhovskikh L M *Volny v Sloistykh Sredakh* (Waves in Layered Media) (Moscow: Izd. AN SSSR, 1957) [Translated into English (New York: Academic Press, 1960)]
38. Rudenko O V, Hedberg C M *Nonlinear Dynamics* **35** (2) 187 (2004)
39. Parton V Z *Mekhanika Razrusheniya*: *ot Teorii k Praktike* (Mechanics of Destruction: from the Theory to Practice) (Moscow: Nauka, 1990)
40. Zarembo L K, Krasil'nikov V A, Shkol'nik I E *Defektoskopiya* **10** 16 (1989); Shkolnik I, Zarembo L, Krasilnikov V, in *Frontiers of Nonlinear Acoustics* (Eds M F Hamilton, D T Blackstock) (London: Elsevier Appl. Sci., 1990) p. 589
41. Shkol'nik I E *Izv. Akad. Nauk SSSR Mekh. Tverd. Tela* 3 (1980)
42. Nilender Yu A, Pochtovik G Ya, Shkol'nik I E *Beton Zhelezobeton* 7 (1969)
43. Robsman V A *Akust. Zh.* **37** 1038 (1991) [*Sov. Phys. Acoust.* **37** 741 (1991)]
44. Robsman V A *Akust. Zh.* **38** 129 (1992) [*Sov. Phys. Acoust.* **38** 112 (1992)]
45. Rabotnov Yu N *Elementy Nasledstvennoi Mekhaniki Tverdykh Tel* (Elements of Hereditary Solid Mechanics) (Moscow: Nauka, 1977) [Translated into English (Moscow: Mir Publ., 1980)]
46. Akhmanov S A, Koroteev N I *Usp. Fiz. Nauk* **123** 405 (1977) [*Sov. Phys. Usp.* **20** 899 (1977)]
47. Johnson P A, Sutin A M, in *Review of Progress in Quantitative Nondestructive Evaluation* Vol. 24 (AIP Conf. Proc., Vol. 760, Eds D O Thompson, D E Chimenti) (Melville, NY: AIP, 2005) p. 377
48. Korobov A I, Izosimova M Yu *Akust. Zh.* (2006) (in press)
49. Rudenko O V, Robsman V A *Akust. Zh.* **50** 836 (2004) [*Acoust. Phys.* **50** 725 (2004)]
50. McCall K R, Guyer R A *Nonlinear Process. Geophys.* **3** 89 (1996)
51. Van den Abeele K E-A et al. *J. Acoust. Soc. Am.* **101** 1885 (1997)
52. Gusev V E, Lauriks W, Thoen J *J. Acoust. Soc. Am.* **103** 3216 (1998)
53. Gusev V E et al. *Wave Motion* **29** 211 (1999)
54. Nazarov V E, Radostin A V *Akust. Zh.* **51** 280 (2005) [*Acoust. Phys.* **51** 230 (2005)]
55. Ostrovsky L A *J. Acoust. Soc. Am.* **116** 3348 (2004)
56. Westervelt P J *J. Acoust. Soc. Am.* **29** 934 (1957)
57. Zverev V A *Akust. Zh.* **45** 685 (1999) [*Acoust. Phys.* **45** 611 (1999)]
58. Beyer R T *Nonlinear Acoustics* 2nd ed. (Woodbury, NY: Acoustical Soc. of America, 1997)
59. Vinogradov N S et al. *Akust. Zh.* **51** 189 (2005) [*Acoust. Phys.* **51** 147 (2005)]
60. Sato T et al. *Ultrasonic Imaging* **7** 49 (1990); in *Frontiers of Nonlinear Acoustics* (Eds M F Hamilton, D T Blackstock) (London: Elsevier Appl. Sci., 1990) p. 98
61. Burov V A et al. *Akust. Zh.* **40** 922 (1994) [*Acoust. Phys.* **40** 816 (1994)]
62. Lapidus Yu R, Rudenko O V *Akust. Zh.* **36** 1055 (1990) [*Sov. Phys. Acoust.* **36** 589 (1990)]
63. Rudenko O V, Soluyan S I *Dokl. Akad. Nauk SSSR* **298** 361 (1988)
64. Volyak K I, Gorshkov A S, Rudenko O V *Vestn. Mosk. Univ. Ser 3 Fiz. Astron.* **17** (1) 32 (1975); Volyak K I *Nelineinye Volny v Okeane. Izbrannye Trudy* (Nonlinear Waves in the Ocean. Selected Works) (Ed.-in-Chief G A Lyakhov) (Moscow: Nauka, 2002) p. 23
65. Rudenko O V, Sarvazyan A P *Biomed. Radioelektron.* (3) 4 (2000) [*Critical Rev. Biomed. Eng.* (3) 6 (2000)]
66. Rudenko O V, Sarvazyan A P, Emelianov S Yu *J. Acoust. Soc. Am.* **99** 2791 (1996)
67. Bailey M R et al. *Akust. Zh.* **49** 437 (2003) [*Acoust. Phys.* **49** 369 (2003)]
68. Rudenko O V *Vestn. Mosk. Univ. Ser. 3 Fiz. Astron.* **37** (6) 1 (1996) [*Moscow Univ. Phys. Bull.* **37** (6) 1 (1996)]
69. Burov V A, Dmitrieva N P, Rudenko O V *Dokl. Ross. Akad. Nauk* **383** 401 (2002) [*Dokl. Biochem. Biophys.* **383** 101 (2002)]
70. Andreev V G et al. *Akust. Zh.* **43** 149 (1997) [*Acoust. Phys.* **43** 123 (1997)]

71. Sarvazyan A P et al. *Ultrasound Med. Biol.* **24** 1419 (1998)
72. Braginsky V B, Mitrofanov V P, Panov V I *Systems with Small Dissipation* (Chicago: Univ. of Chicago Press, 1985)
73. Enflo B O, Hedberg C M, Rudenko O V *J. Acoust. Soc. Am.* **117** 601 (2005)
74. Brysev A P et al. *Akust. Zh.* **50** 725 (2004) [*Acoust. Phys.* **50** 623 (2004)]
75. Preobrazhenskii V L *Usp. Fiz. Nauk* **176** 108 (2006) [*Phys. Usp.* **49** 98 (2006)]
76. Kochina N N, Kochina P Ya, Nikolaevskii V N *Mir Podzemnykh Zhidkostei* (The World of Subterranean Liquids) (Moscow: OIFZ im. O Yu Shmidta RAN, 1994)
77. Nikolaevskii V N *Geomekhanika i Flyuidodinamika* (Geomechanics and Fluid Dynamics) (Moscow: Nedra, 1966)
78. Vil'chinskaya N A *Dokl. Akad. Nauk SSSR* **262** 3 (1982)
79. Dinarev O Yu, Nikolaevskii V N *Akust. Zh.* **51** 623 (2005) [*Acoust. Phys.* **51** 533 (2005)]
80. Sadovskii M A, Nikolaev A V *Seismicheskie Vibratsii na Neftyanykh Mestorozhdeniyakh* (Seismic Vibrations at Oil Fields) (Moscow: IFZ RAN, 1993)
81. Andreev N N *Zh. Prikl. Fiz.* **2** (1 – 2) 205 (1925)
82. Mandel'shtam L I *Lektsii po Kolebaniyam* (Lectures on Vibrations) Vol. 4 (Leningrad: Izd. AN SSSR, 1955) p. 131
83. Landa P S, Duboshinskiĭ Ya B *Usp. Fiz. Nauk* **158** 729 (1989) [*Sov. Phys. Usp.* **32** 723 (1989)]
84. Karlov N V, Kirichenko N A *Kolebaniya, Volny, Struktury* (Vibrations, Waves, Structures) (Moscow: Fizmatlit, 2001)
85. Sobisevich A L, Rudenko O V *Akust. Zh.* **51** (Suppl.) 169 (2005) [*Acoust. Phys.* **51** (Suppl. 1) 149 (2005)]
86. Korobov A I, Brazhkin Yu A, Wang Ning *Akust. Zh.* **51** 663 (2005) [*Acoust. Phys.* **51** 571 (2005)]
87. Tournat V et al. *Akust. Zh.* **51** 633 (2005) [*Acoust. Phys.* **51** 543 (2005)]
88. Mansfeld A D, Mansfeld D A, Reiman A M *Akust. Zh.* **51** 259 (2005) [*Acoust. Phys.* **51** 209 (2005)]